UNIVERSITY OF CALIFORNIA
RIVERSIDE

Regulation of the Rcs Phosphorelay by the Redox Responsive Transcription Factor, OxyR and the Role of a RTX-Like Toxin in Biofilm Formation for the Bacterial Plant Pathogen, *Pantoea stewartii*

A Dissertation submitted in partial satisfaction
of the requirements for the degree of

Doctor of Philosophy

in

Microbiology

by

Polrit Viravathana

September 2022

Dissertation Committee:

Dr. M. Caroline Roper, Chairperson
Dr. Hailing Jin
Dr. Sharon Walker

The Dissertation of Polrit Viravathana is approved:

_____

_____

_____
Committee Chairperson

University of California, Riverside

Acknowledgements

To properly acknowledge everyone properly that made this academic journey possible would make the acknowledgement section longer than the entire dissertation. However, I will do my best in the appropriate amount of space. This research was funded by the Dean's Office of the College of Natural and Agricultural Sciences (CNAS) and the Winter 2020 Graduate Dean's Dissertation Research Grant. Conference travel funding was awarded through multiple Klotz Awards of the Department of Microbiology & Plant Pathology and the UCR Graduate Student Organization Travel Grants. Teaching Assistantships were awarded by the CNAS.

Firstly, I would like to thank my advisor, Caroline Roper for her mentorship, understanding and support. I would like express my most sincere gratitude for allowing me to grow as a scientist in my own way, and always having my back. My successes here and in the future are a result of what I have learned under your tutelage. You have provided me an excellent example for a successful scientist and mentor. Additionally, I would like to acknowledge all the professors who have served on my various committees during my time here at the University of California, Riverside: Sharon Walker, Hailing Jin, Patricia Manosalva, Wenbo Ma, Katherine Borkovich, Linda Walling, and James Borneman. I am thankful and grateful for all your time, help and advice.

Furthermore, no words or writings can describe my gratitude to past and present members of the Roper Lab for your comradery, insights, and for making the lab truly feel like a second home. Whether it is help in experimental ideas and design, writing critique, statistical analysis or just allowing me to vent my frustrations, what I have accomplished

here could not have been done without all your support. As I graduate and depart from this research group to continue my scientific trek, I know that I will follow the lead of many accomplished alumni: Lindsey Burbank, Jeanette Rapicavoli, Brian Ingel, Nichole Ginnan, Claudia Castro, and Biago DiSavlo. To the current members of the Roper Lab: Barbara Jablonska, Alex Blacutt, Flavia Campos Freitas Vieira, Christopher Drozd, Norma Itzel De Anda, Gretchen Heimlich, and Nancy Her, I am forever thankful to be your colleague. To the various undergraduate students who I have mentored at UC Riverside: learning is a two-way street, and I am grateful for the lessons I learned from you as I drilled you through research and academia. Therefore, I would like to recognize Matthew Guevara, Chi Lok Leung, Timothy Smith, Hannah Way, Anisah Kabbara, Rohan Subramanian, and Yona Mizrahi.

Also, I would like to acknowledge the much-appreciated help of those outside the Roper Lab. A special thank you to past and present members of the Manosalva, Walker, Jin and Vidalakis Laboratories, especially Natasha Jackson, Aiden Shands, Daniel White, Baoye He, Sohrab Bodaghi, and Tyler Dang. I would also like to thank Dimitri Niks of the Hille lab in the UCR Department of Biochemistry for his aid in fractionation and ultra-centrifugation. I would like to give recognition to the staff of the UCR Central Facility for Advanced Microscopy and Microanalysis, as well as the UCR Genomics Core for their knowledge and technical expertise. I would especially like to acknowledge and give thanks to David Carter of the UCR Microscopy and Imaging Facility for his guidance and time. Also, I would like to express my gratitude to the administrative staff of the Biochemistry, Microbiology and Plant Pathology, and Nematology Department for

always making sure we had what we needed to get our research done, especially during these unique, and trying times.

Many of my achievements during my doctoral studies would not have been possible without the efforts and support of my skillful collaborators. I would like to recognize Jessica Wen, Jenna Roper and Hideaki Tsutsui of the Tsutsui lab in the UCR Engineering Department, as well as Qiang Sun and Kade Find of the University of Wisconsin, Stevens Point and Yuling Sun at Wellesley College for their expertise in Scanning Electron Microscopy.

In addition, I would like to thank the individuals that encouraged me to step out of my comfort zone and to further my education and capabilities as a scientist. From my days working in the food microbiology and pharmaceutical industry, I would like to acknowledge my former colleagues and mentors: James Knowles and Carlos Martinez of N-Terminus Research Laboratory; Trevor Denbo, Caan Tran, Timothy Chang, Gustavo Acosta, Bridget Baville, Namrata Prasad, Allen Howlett, and Jarrod O'Leary of Med-Pharmex, Inc.; as well as Ha Trinh, Denny Wong and Trevor D'Souza of Cephazone Pharma LLC. Also special thanks to my former colleagues at Toastmasters International Club Number: 7213, District 12, Area A01 (The Master Motivators) for helping me become more comfortable with public speaking.

I am also grateful for my friends and loved ones from Texas Tech University for a place to lay my foundation in academic and molecular biology research. I will always be grateful to Shan L. Bilimoria for taking a chance on a graduate student with an

unorthodox background, as well as Michael San Francisco, Susan San Francisco, Lewis Held, Stephanie Lockwood, Nancy McIntyre, Lou Densmore, Randall Jeter and Zhixin Xie for their patience, and wisdom.

Last, but not least I would like to thank my father, mother, older sister, older brother, friends, and love ones. You never allowed me to give up on myself, and always was patient with my tardiness and/or absence when I was working late in the lab. I always had your compassion, and support, no matter how trying or long the challenge. I will always be forever grateful.

Abstract of the Dissertation

Regulation of the Rcs Phosphorelay by the Redox Responsive Transcription Factor, OxyR and the Role of a RTX-Like Toxin in Biofilm Formation for the Bacterial Plant Pathogen, *Pantoea stewartii*

By

Polrit Viravathana

Doctor of Philosophy, Graduate Program in Microbiology,
University of California, Riverside, September 2022
Dr. M. Caroline Roper, Chairperson

Pantoea stewartii subspecies *stewartii* (*Pnss*) causes Stewart's Wilt in sweet corn and maize, which is characterized by wilting, caused by the formation of exopolysaccharide (EPS)-based biofilms that block the xylem, and the formation of water-soaked lesions. These lesions can form via *Pnss*-induced expression of a repeat-in-toxin (RTX)-like protein called RTX2. Deleting *rtx2* prevents water-soaked lesion formation and effective plant colonization. The *rtx2* gene is in an operon with a second gene that encodes another putative rtx-like toxin (*rtx1*), and two genes that encode the phosphotransferase and the response regulator of the Regulator of Capsular Synthesis (Rcs) phosphorelay, which regulates gene expression via external stimuli. This operon also has a predicted upstream OxyR transcription factor binding site. Water-soaked lesions contain lethal Reactive Oxygen Species (ROS), and previous work by the Roper lab demonstrated that OxyR protects *Pnss* against ROS while deletion of *oxyR* caused increased H_2O_2 sensitivity and negated EPS production. As the operon contains genes for the Rcs phosphorelay, it is

hypothesized that ROS promotes activity of OxyR, thereby inducing gene expression of this operon. Indeed, results of this study show OxyR does bind to the predicted binding site of the *rtx1/rtx2/rcsD/rcsB* operon, and induces its activity. Furthermore, sublethal concentrations of ROS induce gene expression of certain components of the operon in wild type *Pnss*, but not in an *oxyR* deletion mutant. Therefore, ROS appears to be a signal that induces expression of key components of the Rcs phosphorelay via OxyR. The Rcs phosphorelay also plays a key role in cell shape and membrane integrity, and results of this study show that RTX2 affects these cellular characteristics as well, wherein the deletion of *rtx2* causes decreased cell length, increased sensitivity to Polymyxin B, and increased overall cellular hydrophobicity when compared to wild type. RTX2-dependent alteration of the cell envelope also causes increased biofilm formation activity as *Pnss* transitions between the apoplastic and xylem phases of Stewart's Wilt. Furthermore, RTX2 is required for both adhesion and biofilm formation *in-planta*, and impacts biofilm height in a non-EPS producing background (mimicking the initial stages of biofilm formation) *in-vitro*.

Table of Contents

List of Figures

Chapter I

Chapter II

Chapter III

Appendix

List of Tables

Chapter II

Chapter III

Appendix

Chapter I

Introduction

General Introduction

Background

Stewart's wilt of sweet corn is a disease distinguished by water-soaked lesion formation and wilting of corn plants. The causal agent is the bacterium *Pantoea stewartii* subspecies *stewartii*. Stewart's Wilt is endemic to the Ohio River Valley, the Mid-Atlantic regions of the United States, and the southern portion of the Corn Belt (Pataky, 2004). The primary insect vector of *P. stewartii* is the corn flea beetle (*Chaetocnema pulicaria),* found in Canada, and the United States. The bacterium is introduced into the plant via damage caused by insect feeding. Water-soaked lesions will form on the leaves and linear streaks with irregular margins develop parallel to leaf veins. These lesions may extend the entire length of the leaf and become necrotic. *Pantoea stewartii* can also spread to the vascular tissue and form a biofilm in the xylem, that presumably prevents the flow of water and causes wilting of seedlings (Pataky, 2004).

Stewart's wilt is one of the first plant diseases with a developed disease forecast system: winter temperatures influence Stewart's wilt impact during the following spring (Stevens, 1934; Boewe, 1949). Increased winter temperatures increase the severity of Stewart's wilt as more corn flea beetles survive the winter (Pataky, 2004). The development of resistant sweet corn hybrids, has reduced the impact of Stewart's wilt for US domestic corn production, but *Pantoea stewartii* is still a quarantine organism for seed exportation in many other countries (Gehring et al., 2014). Detection of this phytopathogen is performed by ELISA (enzyme-linked immunosorbent assay) or PCR analysis (Wensing et al., 2010). Over 60 countries have import regulations for maize

seeds, while surveillance of traded plant material is required to prevent accidental distribution of *P. stewartii* (Pataky and Ikin 2003). Nonetheless, in 2012 *P. stewartii* causing Stewart's Wilt was reported in Argentina (Orio et al. 2012), and more recently was diagnosed as the causal agent of Jackfruit Bronzing in Malaysia, Indonesia and Mexico (Zulperi et al., 2017, Ibrahim et al. 2020; Rahma et al., 2014; Hernández Morales et al., 2017).

Agent of Stewart's Wilt

Formerly known as *Erwinia stewartii*, *Pantoea stewartii* subsp. *stewartii* is a member of the family Enterobacteriacae within the Gammaproteobacteria. This bacterium is a Gram Negative, rod-shaped, non-spore-forming species. Yellow pigmentation of bacterial colonies can occur depending on which culture medium is used (Pataky, 2004; Mohammadi, et al., 2012).

Following introduction into the corn plant due to feeding by the corn flea beetle, the bacterium colonizes the leaf apoplasts, causing plant cell lysis which results in water-soaked lesions. *P. stewartii* can also directly colonize the xylem tissue. After the appropriate cell densities are achieved, the bacteria form a biofilm encased in a stewartan exopolysaccharide (EPS) matrix, clogging the xylem vessels. Xylem vessel blockage presumably prevents water transport, leading to wilting of the plant (Carlier and Von Bodman, 2006; Von Bodman et al., 1998).

Exopolysaccharide Production and Biofilm Formation

Stewartn EPS is a viscous, high molecular weight polymer (estimated 45 megadaltons) of heptameric oligosaccharide repeat units of glucose, galactose, and glucuronic acid in a 3:3:12 proportion (Huang, 1980; Minogue et al., 2005; Wang et al., 2012). Stewartan EPS production is dependent on a group of 14 genes (designated *cps*) and is regulated in a cell density-dependent manner via quorum sensing (Dolph et al., 1988; Carlier and Von Bodman, 2006; Von Bodman et al., 1998). The quorum sensing regulatory system that controls stewartan EPS production is composed of two genes, *esaI* and *esaR*. EsaI is an acyl-homoserine-lactone (AHL) signal synthase , while EsaR is the cognate transcription factor (Von Bodman, et al. 1998; Carlier and Von Bodman, 2006). Unlike quorum sensing systems in many other bacterial species that act as inducers, *P. stewartii* EsaR represses EPS synthesis by binding to promoter regions as a dimer in the absence of AHL. This repressor activity prevents expression of the *cps* genes at low cell density (low AHL). De-repression of the *cps* genes and increased EPS production requires higher concentrations of AHL (indicative of high cell density) which lead to reduced binding of EsaR and de-repression of EPS synthesis (Von Bodman and Farrand, 1995; Von Bodman, et al. 1998). Quorum sensing also regulates proper biofilm development, adhesion and host colonization of *P. stewartii* in sweet corn seedlings (Koutsoudis et al., 2006; Rumbaugh and Armstrong, 2014). Specifically, mutants constitutively expressing EPS yield loose biofilms and are reduced in virulence, indicating that coordination of EPS production and biofilm formation in *P. stewartii* is necessary for plant infection (Koutsoudis et al., 2006).

The Regulator of Capsular Synthesis (Rcs) Phosphorelay

The regulator of capsular synthesis (Rcs) phosphorelay is a complex, bacterial signal transduction system that translates environmental stimuli to alter gene expression. Found only in the family Enterobacteriaceae, activation of the Rcs phosphorelay is caused by a variety of conditions including changes in environment (i.e., growth on solid surfaces or at low temperatures), and exposure to polymyxin B, a compound that disrupts cellular envelope components (Huang et al., 2006; Pescartetti et al., 2013). First described in *Escherichia coli*, the Rcs phosphorelay was primarily known for control of the *cps* operon (operon managing synthesis of capsular polysaccharide colonic acid; Majdalani and Gottesman, 2005) the Rcs system also regulates genes vital for protection against oxidative stress, as well as bacterial cell wall integrity (Andresen, et al., 2007; Latasa, et al., 2012; Farizano et al., 2014). Activation can also be induced by perturbations or modifications to the bacterial membrane, or overproduction of certain membrane bound proteins (DjlA, YpdI, LolA and OmpG; Hinchliffe, et al., 2008; Madec et al., 2014). Once activated, the Rcs system regulates many different cellular processes, including aspects of the cellular envelope, biofilm formation, cell division and control of flagellar genes and virulence factors (Hinchliffe et al., 2008). The Rcs phosphorelay also has a significant role in governing cell shape and regulating cell division (Ranjit and Young, 2013; Luo et al., 2015).

The phosphorylation of well conserved histidine (H) and aspartic acid (D) amino acid residues are key to activation of the Rcs regulatory system. The proteins involved in this network are the transmembrane sensor kinase (RcsC), transmembrane intermediary

protein (RcsD, also known as YojN), and the cytoplasmic response regulator (RcsB). RcsF is an outer membrane lipoprotein that can increase autophosphorylation activity of RcsC by some unknown mechanism (Majadalani and Gottesman, 2005; Huang et al., 2006; Hinchliffe, et al. 2008).

Stimulus of the Rcs system leads to autophosphorylation of the histidine kinase domain (H1) of RcsC. The phosphate is then transferred to a conserved aspartic acid in the receiver domain (D1) of the same protein (Majdalani and Gottesman, 2005; Pescartetti, et al., 2013), then to H2 of the RcsD histidine phosphotransfer domain (HPt), and then to the D2 receiver domain of the cytoplasmic protein RcsB (Majadalani and Gottesman, 2005; Farizano et al., 2014). Active (phosphorylated) RcsB may form a homodimer or a heterodimer with the auxiliary response regulator RcsA, and these complexes bind to different promoter sequences. As a heterodimer with RcsA, the RcsBA protein complex regulates the *cps* operon and other capsule related genes by binding to a promoter sequence (known as the "RcsAB box") which has the consensus sequence: TaAGaatatCctA. This regulatory sequence has a tenfold higher binding affinity for the RcsA-RcsB heterodimer vs. RcsB alone (Pristovsek et al., 2003). In *P. stewartii*, RcsA is also regulated by the EsaI/EsaR quorum sensing system. Expression of *rcsA* is repressed by EsaR at low cell concentration, and as cell density increases, EsaR repression is released (Von Bodman et al. 1998; Minogue et al., 2005).

Genome organization of major components of the Rcs phosphorelay is conserved among members of the family Enterobacteriaceae. In order, genes *rcsD* and *rcsB* are adjacent, with *rcsC* downstream in the opposite orientation (Dehal, et al. 2009). In

Salmonella species, *rcsD* and *rcsB* are in their own operon, and expression of *rcsB* is controlled by two different promoters. Higher expression of *rcsB* negatively impacts expression of *rcsD* (Pescaretti et al., 2010). However, in the genome of *P. stewartii*, two genes encoding separate RTX toxins are located upstream of *rcsD* and *rcsB*. Designated *rtx1* and *rtx2*, all 4 genes (*rtx1-rtx2-rcsD-rcsB*) may be transcribed as a single operon (Burbank 2014; Roper, unpublished data).

Repeat-in-Toxins

A major contributing factor to formation of water-soaked lesions during *P. stewartii* plant infection is the unique, repeat-in-toxin (RTX) like protein designated RTX2 (Roper et al., 2015). Repeat in toxin (RTX) proteins are a group of large proteins (40 to 600+ kDa) characterized by glycine-aspartate (GD)-rich peptide repeats (G-G-X-G-(N/D)-D-X-(L/I/V/W/Y/F)-X where X can be any amino acid near the C-terminus (Ostolaza et al., 2019; Satchell 2011). Each repeat forms half of a portion of a ß-roll structure with a GGxG consensus forming the tight turn followed by a β-strand. A hydrophobic interior is formed by hydrophobic residues in the ß-roll structure. A calcium ion is located in each turn, which is bound to a conserved aspartate in the sixth position of the repeat (Satchell, 2011). These Ca^{2+} binding domains are vital for proper folding and activity of RTX toxins once these proteins are exported to the cell surface (Fiser and Konopasek, 2009; Chenal *et al*., 2010; Satchell, 2011). Most, but not all, RTX toxins are secreted via a Type I secretion system. Requirements for RTX toxin Type 1-secreted export are an inner membrane ATPase, transmembrane periplasmic linker protein, and a TolC, or TolC-like outer membrane porin (Chenal et al., 2010; Satchell, 2011).

Repeat-in-toxins include the 117 kDa, alpha (α) hemolysin from *Escherichia coli* (HlyA) and the adenylate cyclase toxin from *Bordetella pertussis*. The *E. coli* originating toxin lyses erythrocytes by colloid osmotic shock by forming hydrophilic pores in the cell wall, the latter toxin can damage bacterial membranes without using specific cellular receptors and forms small-cation selective membrane channels, flooding the interior of the host cell with monovalent cations, leading to osmotic lysis (Menestrina, et al., 1994; Fiser and Konopasek, 2009). One of the most diverse and largest groups of RTX proteins are the large repetitive RTX adhesins.

Collectively categorized into a broader group called Biofilm associated proteins (BAP), these proteins often function as adhesins, proteins which are often loosely attached to the cell envelope and play a role in biofilm development (Satchell, 2011; Lasa and Penades, 2006). Known for their large size, and the classical nonapeptide repeats at their C-terminus, these proteins are also distinguished for having 80 – 300 amino acid long extensive tandem repeats that vary in number and length between species (Girard and Mourez, 2006; Satchel 2011). Some of the most well characterized BAP proteins are the LapA and LapF proteins of *Pseudomonas putida*. Both of these proteins are large (8682 and 6310 amino acids in length), and are vital to the three-dimensional architecture of the biofilm: LapA is required for irreversible attachment to surfaces while LapF is needed for cell to cell interaction (Satchel, 2011). The SiiE protein from *Salmonella enterica* is a repetitive RTX protein needed for the colonization of cattle intestine. While its gene is found on *Salmonella* pathogenicity island 4 (SPI-4), SiiE is loosely localized to the surface and is an adhesin which attaches to epithelial cells (Satchell, 2011).

Other Virulence Factors

Plant Cell Wall Degrading Enzymes

Plant Cell Wall Degrading Enzymes are key components of a plant pathogen's arsenal: use of these proteins promotes pathogen movement through the plant xylem, as these enzymes break down components of the plant cell wall (Roper et al., 2007; Ingel et al., 2019) An endogluconase, EngY, from *P. stewartii* is a O-glycosyl hydrolase that cleaves the glycosydic bond between a carbohydrate and a noncarbohydrate component or between two or more carbohydrates (Mohammadi et al., 2011). This enzyme degrades carboxymethyl cellulose, β-D-glucan, and xylan, and its deletion (*ΔengY*) results in *P. stewartii* losing all endoglucanase and xylanase activity *in vitro*. *In planta, P. stewartii ΔengY* is compromised in movement within the xylem vessels and as a result, this mutant causes less wilting in corn seedlings (Mohammadi et al., 2011).

Type III Secretion Systems

Pantoea stewartii has two Type III Secretion Systems (T3SS) (Correa et al., 2012; Walterson, and Stavrinides, 2015). One of the T3SS in *P. stewartii* is involved in colonizing its insect host (Correa et al., 2012). The bacterium can be found in the foregut, midgut, and hindgut of *C. pulicaria* up to 12-days post-acquisition (Ammar *et al*., 2014). For infection of plants, *P. stewartii* relies on a Hrp T3SS encoded by the 29-kb, *hrp* gene cluster with 8 complementation groups (Ahmad *et al*., 2001; Roper, 2011). The bacterium's effector locus contains two genes, *wtsE* and *wtsF* (Roper, 2011). WtsE is a 201 kDa protein belonging to the AvrE family of effector proteins (Ham et al., 2006; Roper, 2011) and WtsF is a molecular chaperone of WtsE (Ham et al., 2006). AvrE-

family effector proteins are widely conserved in plant-pathogenic bacteria and are characterized by one, to two WxxxE motifs and a putative C-terminal endoplasmic reticulum membrane retention/retrieval signal (ERMRS). Similar to the effector DspE (aka DspA) of *Erwinia amylovora*, the WtsE protein is an essential pathogenicity factor for *P. stewartii* (Ham et al., 2009). Eliciting a hypersensitive response (HR; where cells immediately surrounding the site of infection rapidly die) in susceptible hosts, this cytotoxin causes water-soaked lesions and suppresses host defense systems, but in non-susceptible hosts, this effect can still illicit an efficient hypersensitive response (HR) response (Tampakaki and Panopoulos, 2000; Ham et al., 2008; 2009).

Pantoea stewartii also produces harpins. Harpins are glycine-rich proteins that are also secreted through the Type III secretion system. These proteins also have few aromatic amino acid and cysteine residues. Harpins are protease sensitive but heat stable, despite having little or no cysteine residues (two cysteine residues are required for disulfide bond formation; Ahmad et al., 2001; Choi et al., 2013). Unlike effectors, harpins appear to be targeted to the plant tissue extracellular space by plant-pathogenic bacteria (Choi et al., 2013). Similar to harpins of other *Erwinia* species the *hrpN* gene from *P. stewartii* encodes a protein 382 amino acids in length (Ahmad et al., 2001). The harpin from *P. stewartii* can elicit a HR in tobacco, but a mutation in *hrpN* does not change the virulence of this bacterium in sweet corn. This suggests that the harpin of *Pantoea stewartii* subspecies stewartii may have an insignificant role in its virulence (Ahmad et al., 2001).

Motility

Surface motility is vital for *P. stewartii* colonization of the plant host. This motility is flagella-dependent on semisolid media and requires production of exopolysaccharide. Surface-based motility is also influenced by active sideophore-dependent iron acquisition. Deletion of either the *iucA* (aerobactin siderophore biosynthesis) or *iutA* (siderophore transport) genes disrupts surface motility and limits movement in planta (Burbank et al. 2015). *P. stewartii* has not been observed to engage in, but cannot swim with motility in aqueous environments (Herrera et al. 2008).

Regulating Oxidative Stress

During its infection cycle, *Pantoea stewartii* encounters significant amounts of reactive oxygen species (ROS). Chemicals, such as H_2O_2 and superoxides, are part of the plant's innate immune system, serving as signaling molecules and components of the plant defense response (Choi et al., 2007; Yadeata and Tomma, 2013; Hilaire et al., 2001). Water-soaked lesions which develop during infection also contain significant amounts of ROS (Burbank and Roper, 2014). Therefore *P. stewartii* must have a strategy to combat this environment.

Transciption factor OxyR

The transcription factor OxyR is a thiol-based redox sensor that aids in maintaining the proper redox state inside the bacterial cell by transcriptionally activating genes that yield enzymes for protection against oxygen radicals (Tao et al., 1991; Green and Paget, 2004). A member of the LysR family of transcriptional regulators, this enzyme has a helix-turn-helix DNA-binding motif (HTH) at its N-Terminal domain and contains

6 cysteine thiols that directly monitor the oxidative environment in the cell (Zheng and Storz, 2000; Green and Paget, 2004).

Forming a tetramer in solution, this 34 kDa protein is inactive in its reduced form. When the cell is under oxidative stress, OxyR is oxidized; the conserved cysteine residues form disulfide bonds, activating this transcription factor (Seo et al., 2015; Zhang and Storz, 2000). The *oxyR* gene is negatively regulated by its protein product (Tao et al., 1991). The primary purpose of the OxyR system is to combat negative effects of hydrogen peroxide (Tao et al., 1991; Seo et al., 2015; Burbank and Roper, 2014; Yu et al. 2016). Mutations in *oxyR* result in increased sensitivity to hydrogen peroxide in many bacterial species (Tao et al., 1991; Burbank and Roper; 2014; Yu et al., 2016). Deletion of *oxyR* in *P. stewartii* also leads to the inability of the bacterium to produce EPS, although the mechanism is unknown (Burbank and Roper et al., 2014).

Carotenoid Pigment Production

*Pantoea stewart*ii subspecies *stewartii* produces a yellow carotenoid pigment. This naturally occurring chemical absorbs light in the 400 – 550 nm wavelength, resulting in *P. stewartii*'s distinct yellow to orange color. Deletion of *crtB* (encode for Phytoene synthase, enzyme in the first step of carotenoid synthesis) results in loss of pigment production in *P. stewartii*. In addition to loss of tolerance to UV radiation, the *crtB* mutant is also impaired in virulence, and is more sensitive to H_2O_2 when compared to wild type *P. stewartii*. (Mohammadi et al., 2012). Carotenoids provide protection against ROS by quelling singlet molecular oxygen and peroxyl radicals (Stahl and Sies, 2003).

Dissertation Purpose and Justification

Biofilm formation allows the bacterium to survive against the host plant environment. This adaptation allows bacterial communities to withstand environmental challenges, but requires the tightly regulated synthesis of exopolysaccharide (EPS; Burbank and Roper, 2014). Identification of what triggers this defensive mechanism may give insight to how to combat biofilms during infection processes. The Rcs phosphorelay is required for EPS production in *P. stewartii*, but it is not known what exogenous environmental factor(s) induces expression or activity of this important and complex signal transduction system. The primary purpose of this research is to determine if ROS may act as an external environmental signal that induces the process of biofilm formation in *P. stewartii* via the Rcs phosphorelay by use of the transcription factor OxyR.

A conserved DNA binding site for OxyR is predicted upstream of the operon containing *rcsD* and *rcsB* along with two RTX-like proteins (Burbank, 2014; Roper, unpublished data). Deletion of the smaller RTX gene (designated *rtx1*) yields no change in phenotype, but deletion of the larger toxin gene (*rtx2*) decreases virulence, reduces exopolysaccharide (EPS) production, and significantly reduces formation of water-soaked lesions in corn seedlings (Roper et al., 2015; Roper, unpublished data). These water-soaked lesions contain ROS (i.e. H_2O_2 and superoxides; Burbank and Roper, 2014). In addition to its role in forming water-soaked lesions, RTX2 may serve an additional function in *Pantoea stewartii*: to alter membrane dynamics and initiate biofilm formation to protect the bacterium from ROS in the surrounding environment (Figure 1.1). The

unique RTX2 protein shares similarities with other RTX proteins, yet it cannot be categorized into a specific subfamily of RTX proteins (Roper *et al*., 2015).

Therefore, I hypothesize that presence of ROS acts as an environmental signal that induces expression of key components of the Rcs signal transduction system via the transcription factor OxyR, and uses RTX2-dependent alteration of the bacterial membrane properties to stimulate phosphotransfer through the Rcs system. This coordinated response would allow for increased EPS production and biofilm formation, as *P. stewartii* transitions between the apoplastic and xylem phases of Stewart's Wilt (Figure 1.1).

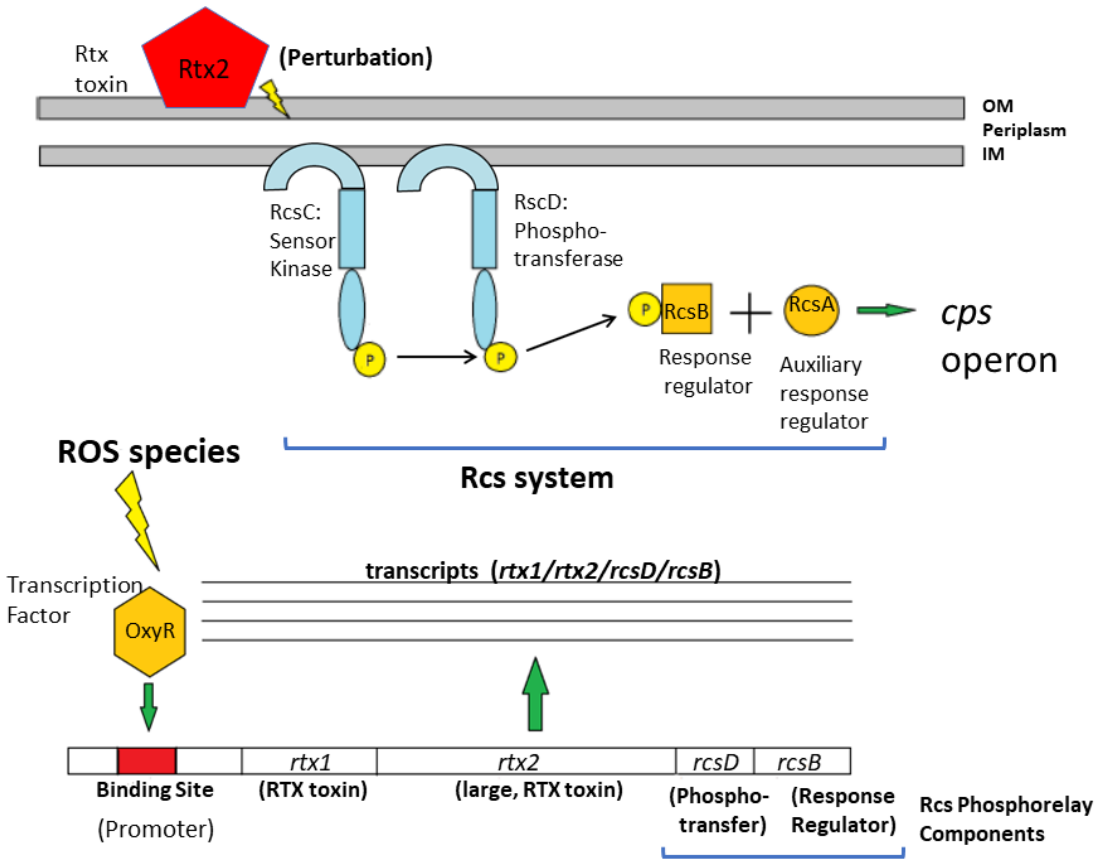
Rtx
toxin
Rtx2
(Perturbation)
OM
Periplasm
IM
RcsC:
Sensor
Kinase
RscD:
Phospho-
transferase
P
RcsB
RcsA
Response
regulator
Auxiliary
response
regulator
cps
operon
ROS species
Rcs system
Transcription
Factor
OxyR
transcripts (rtx1/rtx2/rcsD/rcsB)
rtx1
rtx2
rcsD
rcsB
Binding Site
(Promoter)
(RTX toxin)
(large, RTX toxin)
(Phospho-
transfer)
(Response
Regulator)
Rcs Phosphorelay
Components

Figure 1.1. **Proposed Model for relationship between OxyR, RTX2 and the Rcs phosphorelay**. ROS species induces gene expression of an operon containing two genes encoding for RTX-like toxins (designated *rtx1* and *rtx2*) and two genes for certain components of the Rcs phosphorelay (the phosphotransfer receptor RcsD and the terminal response regulator RcsB). Integration and perturbation of the RTX2 protein in the cell envelope yield increased activity in the Rcs phosphorelay. Phosphorylation of the sensor kinase RscC activates this protein. RcsC phosphorylates RcsD, the phosphotransfer protein, which then phosphorylates the cytoplasmic response regulator RcsB. Now active phosphorylated RcsB forms a heterodimer with the auxiliary response regulator RcsA to induce expression of the *cps* operon, yielding EPS for biofilm formation (Minogue *et al*., 2005; Function of genes in operon are in parentheses; Abbreviations: OM = Outer Membrane, IM = Inner membrane, small yellow circle with a P indicates a phosphate group, black arrows denote transfer of phosphate group).

Literature Cited

Ahmad, M., Majerczak, D.R., Pike, S., Hoyos, M.E., Novacky, A., and Coplin D.L. 2001. Biological activity of harpin produced by *Pantoea stewartii* subsp. *stewartii*. *Molecular Plant Microbe Interactions* 10(14): 1223-1234.

Ammar, E., Correa, V.R., Hogenhouta, S.A., and Redinbaugh, M.G. 2014. Immunofluorescence localization and ultrastructure of Stewart's wilt disease bacterium *Pantoea stewartii* in maize leaves and in its flea beetle vector *Chaetocnema pulicaria* (Coleoptera: Chrysomelidae) *Journal of Microscopy and Ultrastructure* 2: 28–33

Andresen, L., Koiv, V., Alamäe, T., and Mäe, A. 2007. The Rcs phosphorelay modulates the expression of plant cell wall degrading enzymes and virulence in *Pectobacterium carotovorum* ssp.*carotovorum*. *FEMS Microbiology Letter*: 229–238

Boewe, G. H. 1949. Late season incidence of Stewart's disease on sweet corn and winter temperatures in Illinois, 1944-1948. *Plant Disease Report* 33:192-194.

Burbank, L. and Roper, M.C. 2014. OxyR and SoxR Modulate the Inducible Oxidative Stress Response and Are Implicated During Different Stages of Infection for the Bacterial Phytopathogen *Pantoea stewartii* subsp. *stewartii*. *Molecular Plant-Microbe Interactions* 27(5): 479-490.

Burbank, L. 2014. Global Regulation of Virulence Determinants During Plant Colonization in the Bacterial Phytopathogen, *Pantoea stewartii* subsp. *stewartii*. Doctoral Dissertation.

Burbank L, Mohammadi M, and Roper MC. 2015. Siderophore-mediated iron acquisition influences motility and is required for full virulence of the xylem dwelling bacterial phytopathogen *Pantoea stewartii* subsp. *stewartii*. *Applied Environmental Microbiology* 81:139 –148. doi:10.1128/AEM.02503-14

Carlier, A.L. and Von Bodman, S.B. 2006. The rcsA promoter of *Pantoea stewartii* subsp. *stewartii* features a low-level constitutive promoter and an EsaR Quorum-Sensing-Regulated Promoter. *Journal of Bacteriology* 188(12): 4581-4584.

Chenal, A, Karst, J.C., Perex, A.C.S. Wozniak, A.K., Baron, B., England, P. and Landant, D. 2010. Calcium-Induced Folding and Stabilization of the Intrinsically Disordered RTX Domain of the CyaA Toxin. *Biophysical Journal* 99: 3744-3753.

Choi, H.W., Kim, Y.J., Lee, S.C., Hong, J.K., Hwang, B.K. 2007. Hydrogen Peroxide Generation by the Pepper Extracellular Peroxidase $CaPO_2$ Activates Local and Systemic Cell Death and Defense Response to Bacterial Pathogens. *Plant Physiology* 145: 890-904.

Choi, M., Kim, W., Lee, C. and Oh, C. 2013. Harpins, Multifunctional Proteins Secreted by Gram-Negative Plant-Pathogenic Bacteria. *Molecular Plant Microbe Interactions* 26(10): 1115-1122.

Correa, V.R., Majerczak, D.R., Ammar, E., Merighi, M., Pratt, R.C., Hogenhout, S.A., Coplin, D.L., and Redinbaugh, M.G. 2012. The Bacterium *Pantoea stewartii* uses two different Type III Secretion Systems to colonize its Plant Host and Insect Vector. *Applied and Environmental Microbiology* 78(17): 6327-6336

Dehal, P. S., Joachimiak, M. P., Price, M. N., Bates, J. T., Baumohl, J. K., Chivian, D., Friedland, G. D., Huang, K. H., Keller, K., Novichkov, P.S., Dubchak, I. L., Alm, E. J., and Arkin, A. P. 2009. MicrobesOnline: an integrated portal for comparative and functional genomics. *Nuc. Acids Res*. DOI: 10.1093/nar/gkp919

Dolph, P.J., Majerczak, D.R. and Coplin, D.L. 1988. Characterization of a gene cluster for exopolysaccharide biosynthesis and virulence in *Erwinia stewartii*. *Journal of Bacteriology* 170, 865–871.

Farizano, J.V., Torres, M.A., Pescaretti, M.M., and Delgado, M.A. 2014. The RcsCDB regulatory system plays a crucial role in the protection of *Salmonella enterica* serovar *Typhimurium* against oxidative stress. *Microbiology* 160: 2190-2199.

Fiser, R., and Konopasek, I. 2009. Different modes of membrane permeabilization by two RTX toxins: Hyla from *Escherichia coli* and CyaA from *Bordatella pertussis*. *Biochimica et Biophysica Acta* 1788: 1249-1254.

Gehring, I., Wensing, A., Gernold, M., Wiedemann, W. Coplin, D.L., and Geider, K. 2014. Molecular differentiation of *Pantoea stewartii* subsp. i*ndologenes* from subspecies *stewartii* and identification of new isolates from maize seeds. *Journal of Applied Microbiology* 116: 1553 -1562

Girard, V., and Mourez, M. 2006. Mini-review: Adhesion mediated by autotransporters of Gram-negative Bacteria: Structural and functional features. *Research in Microbiology* 157: 407-116

Green, J., and Paget, M.S. 2004. Bacterial Redox sensors. *Nature* 2: 954-967.
Grellet-Bournonville, C.F.G., and Díaz-Ricci, J.C. 2011. Quantitative Determination of Superoxide in Plant Leaves Using a Modified NBT Staining Method. *Phytochemical Analysis* 22: 268–271

Ham, J.H., Majerczak, D.R., Arroyo-Rodriguez, A.S., Mackey, D.M., and Coplin D. 2006. WtsE, and AvrE-family effector protein from *Pantoea stewartii* subsp. *stewartii*, causes disease-associated cell death in corn and requites a chaperone protein for stability. *Molecular Plant Microbe Interactions* 19: 1092-1102.

Ham, J.H., Majerczak, D., Ewert, S., Sreerekha, M., Mackey, M., and Coplin, D. 2008. WtsE, an AvrE-family type III effector protein of *Pantoea stewartii* subsp. *stewartii*, causes cell death in non-host plants. *Molecular Plant Microbe Interactions* 9:633-643.

Ham, J.H., Majerczak, D.R., Nomura, K., Mecey, C., Uribe, F., He, S., Mackey, D., and Coplin D.L. 2009. Multiple Activities of the Plant Pathogen Type III Effector Proteins WtsE and AvrE Require WxxxE Motifs. *Molecular Plant Microbe Interactions* 22(6): 703–712.

Hernández-Morales, A., Pérez-Casillas, J.M., Soria-Guerra, R.E., VelázquezFernández, J.B., and JArvizu-Gómez, J.L. 2017. First report of *Pantoea stewartii* subsp. *stewartii* causing jackfruit bronzing disease in Mexico. *Journal of Plant Pathology* 99(3).

Herrera, C. M., Koutsoudis, M. D.,Wang, X., and Von Bodman, S. B. 2008. *Pantoea stewartii* subsp. *stewartii* exhibits surface motility, which is a critical aspect of Stewart's wilt disease development on maize. *Molecular Plant Microbe Interactions*. 21:1359-1370.

Hilaire, E., Young, S.A., Willard, L.H., McGee, J.D., Sweat, T., Chittor, J.M., Guikema, J.A., and Leach, J.E. 2001. Vascular Defense Responses in Rice: Peroxidase Accumulation in Xylem Parenchyma Cells and Xylem Wall Thickening. *Molecular Plant-Microbe Interaction* 14(12): 1411-1419.

Hinchliffe S.J., Howard S.L., Huang Y.H., Clarke D.J., Wren B.W. 2008. The importance of the Rcs phosphorelay in the survival and pathogenesis of the enteropathogenic *Yersiniae*. *Microbiology* 154:1117–1131

Huang, J. 1980. Galactosyltransferase activity in *Erwinia stewartia* and its role in biosynthesis of extracellular polysaccharide. *Physiological Plant Pathology*. 17:73-80.

Huang, Y., Ferrieres, L., and Clarke, D.J. 2006. The role of the Rcs phosphorelay in *Enterobacteriaceae*. *Research in Microbiology* 157: 206-212.

Ibrahim, R , Ismail-Suhaimy, N.W., Shu-Qing, T., Ismail, I., Abidin, N., Mansor, H., & Karam, D.S., Ahmad-Hamdani, M.S., Yusof, M.T., and Zulperi, D. 2020. Molecular characterization and phylogenetic analysis of *Pantoea stewartii* subspecies *stewartii* causing bronzing disease of jackfruit in Malaysia based on *cps* and *hrp* gene sequences. *Journal of Plant Pathology* 102: 193 - 199

Ingel, B., Jeske, D.R., Sun, Q., Grosskopf, J., and Roper M.C. 2019. *Xylella fastidiosa* Endoglucanases Mediate the Rate of Pierce's Disease Development in *Vitis vinifera* in a Cultivar-Dependent Manner. *Molecular Plant-Microbe Interaction* 32(10)

Koutsoudis, M.D., Tsaltas, D., Minogue, T.D., and Von Bodman, S.B. 2006. Quorum-sensing regulation governs bacterial adhesion, biofilm development, and host colonization in *Pantoea stewartii* subspecies *stewartii*. *Proceedings of the National Academy of Sciences* 103: 15 5983-5988

Lasa, I., and Penadés, J.R. 2006. Mini-Review: Bap: A family of surface proteins involved in biofilm formation. *Research in Microbiology* 157: 99–107

Latasa, C., Garcia, B., Echeverz, M., Toledo-Arana, A., Valle, J., Campoy, S., Garcia-del Portillo, F., Solano, C., and Lasa, I. 2012. *Salmonella* Biofilm Development Depends on the Phosphorylation Status of RcsB. *Journal of Bacteriology* 194(14): 3708-3722.

Luo, I, Wiebe, J. and Liu, Y. 2015. The Rcs Phosphorelay May Regulate the *E. coli* Capsule Response to Sublethal Streptomycin Treatment. *Journal of Experimental Microbiology and Immunology (JEMI*).

Madec, E., Bontemps-Gallo, S. and Lacroix, J. 2014. Increased phosphorylation of the RcsB regulator of the RcsCDB phosphorelay in strains of *Dickeya dadantii* devoid of osmoregulated periplasmic glucans revealed by Phos-tag gel analysis. *Microbiology* 160: 2763-2770

Majdalani N., and Gottesman S. 2005. The Rcs Phosphorelay: A Complex Signal Transduction System. *Annual Review of Microbiology* 59: 379-405

Menestrina, G., Moser, C., Pellet, S., and Welch, R. 1994. Pore-formation by *Escherichia coli* hemolysin (HlyA) and other members of the RTX toxins family. *Toxicology* 87(1-3): 249-267. doi: 10.1016/0300-483x(94)90254-2

Minogue, T.D., Carlier, A.L., Koutsoudis, M.D., and Von Bodman, S.B. 2005. The cell density-dependent expression of stewartan exopolysaccharide in *Pantoea stewartii* ssp. *stewartii* is a function of EsaR-mediated repression of the *rcsA* gene. *Molecular Microbiology* 56(1): 189-203.

Mohammadi, M., Burbank, L. and Roper, M.C. 2011. *Pantoea stewartii* subsp. *stewartii* Produces an Endoglucanase That Is Required for Full Virulence in Sweet Corn. *Molecular Plant-Microbe Interaction* 25(4) 2012, pp. 463–470

Mohammadi, M., Burbank, L., and Roper, M.C. 2012. Biological Role of Pigment Production for the Bcaterial Phytopathogen *Pantoea stewart*ii subsp. *stewartii*. *Applied and Environmental Microbiology* 78(19): 6859-6865.

Orio, G.A., Brücher, E., Plazaz, M.C., Sayago, P., Guerra, F., Rossi, R.D., Ducasse, D.A., Guerra, G.D. 2012. Disease Notes: First Report of Stewart's Wilt of Maize in Argentina Caused by *Pantoea stewartii. Plant Diseases* 96 (12): 1819.3 -1819.3

Ostolaza, H., Gonzalez-Bullon, D., Uribe, K.B., Martin, C. Amuategi, J., and Fernandez-Martinez, X. 2019. Review: Membrane Permeabilization by Pore Forming RTX toxins: What kind of Lesions do these toxins form? *Toxins* 11(6) 354

Pataky, J., and Ikin, R. 2003. Pest risk analysis: the risk of introducing *Erwinia stewartii* in maize seed. The International Seed Federation, Nyon, Switzerland

Pataky, J.K. 2004. Stewart's wilt of corn. In: The Plant Health Instructor. doi:10.1094/PHI-I-2004-0113-01. Published online.

Pescaretti, M.d.M., Lopez, F.F., Morero, R.D., and Delgado, M.A. 2010. Transcriptional autoregulation of the RcsCDB phosphorelay system in *Salmonella enterica* serovar *Typhimurium*. *Microbiology* 156: 3513–3521

Pescaretti, M.d.M., Farizano, J.V., Morero, R., Delgado, M.A. 2013. A Novel Insight on Signal Transduction Mechanism of RcsCDB System in *Salmonella enterica* Serovar *Typhimurium*. PLoS ONE 8(9): e72527. doi:10.1371/journal.pone.0072527

Pristovsek P, Sengupta K, Lohr F, Schafer B, Von Trebra M.W., Ruterjans, H. and Bernhard, F. 2003. Structural analysis of the DNA-binding domain of the *Erwinia amylovora* RcsB protein and its interaction with the RcsAB box. *Journal of Biological Chemistry* 278:17752–59

Rahma, H., Sinaga, M.S., Surahman, M., and Giyanto. 2014. First Report of Stewart's Wilt of maize caused by *Pantoea stewartii* subsp. *stewartii* in Bogor District, Indonesia. J.ISSAAS 20(2): 131 – 141.

Ranjit, D.K., and Young, K.D. 2013. The Rcs Stress Response and Accessory Envelope Proteins Are Required for De Novo Generation of Cell Shape in *Escherichia coli*. *Journal of Bacteriology* 195(11): 2452-2462

Roper, M.C., Greve, L.C., Warren, J.G., Labavitch, J.M., and Kirkpatrick, B.C. 2007. *Xylella fastidiosa* Requires Polygalacturonase for Colonization and Pathogenicity in *Vitis vinifera* Grapevine. *Molecular Plant-Microbe Interaction* 20(4) 411-419.

Roper, M.C. 2011. *Pantoea stewartii* subsp. *stewartii*: lessons learned from a xylem-dwelling pathogen of sweet corn. *Molecular Plant Pathology* 12(7): 628–637.

Roper, M.C., Burbank, L.P., Williams, K., Viravathana, P., Tien, H. and Von Bodman, S. 2015. A large repetitive RTX-like protein mediates water-soaked lesion development, leakage of plant cell content and host colonization in the *Pantoea stewartii* subsp. *stewartii* pathosystem. *Molecular Plant-Microbe Interactions* 12: 1374-1882.

Rumbaugh KP and Armstrong A. “The Role of Quorum Sensing in Biofilm Development”, in Rumbaugh, K.P. and Ahmad, I. (eds). Antibiofilm Agents: From diagnosis to treatment and prevention (Springer Series on Biofilms) pgs.97-113. 2014. Springer, Humana Press, New York, NY. ISBN: 978-3-642-53832-2

Satchell, K.J.F. 2011. Structure and Function of MARTX Toxins and other large repetitive RTX proteins. *Annual Review of Microbiology* 65: 71-90

Seo, S.W., Kin, D., Szubin, R., and Palsson, B.O. 2015. Genome-wide Reconstruction of OxyR and SoxRS Transcriptional Regulatory Networks under Oxidative Stress in *Escherichia coli* K-12 MG1655. *Cell Reports* 12: 1289-1299.

Stahl, W., and Sies, H. 2003. Antioxidant activity of carotenoids. *Molecular Aspect of Medicine* 24(6): 345-351.

Stevens, N. E. 1934. Stewart's disease in relation to winter temperatures. *Plant Dis. Rep. 18:141-149*

Tampakaki, A. P., and Panopoulos, N. J. 2000. Elicitation of hypersensitive cell death by extracellularly targeted HrpZPsph produced in planta. *Molecular Plant-Microbe Interactions*. 13:1366-1374

Tao, K., Makino, K., Yonei, S., Nakata, A., and Shinagawa, H. 1991. Purification and Characterization of the *Escherichia coli* OxyR Protein, the Positive Regulator for a Hydrogen Peroxide-Inducible Regulon. *Journal of Biochemistry* 109: 262-266.

Von Bodman, S. and Farrand, S.K. 1995. Capsular polysaccharide biosynthesis and pathogenicity in *Erwinia stewartii* require induction by an N-acylhomoserine lactone autoinducer. *Journal of Bacteriology* **177**, 5000–5008

Von Bodman, S., Majerczak, D.R., and Coplin, D.L. 1998. A negative regulator mediates quorum-sensing control of exopolysaccharide production in *Pantoea stewartii* subsp. *stewartii*. *Proceedings of the National Academy of Sciences* 95: 7687-7692

Walterson, A.M., and Stavrinides, J. 2015. *Pantoea*: insights into a highly versatile and diverse genus within the Enterobacteriaceae. *FEMS Microbiology Reviews*: fuv027.

Wang, X., Yang, F., and Von Bodman, S.B. 2012. The genetic and structural basis of two distinct terminal side branch residues in stewartan and amylovoran exopolysaccharides and their potential role in host adaptation. *Molecular Microbiology* 83: 195-207

Wensing, A., Zimmermann, S. and Guider, K. 2010. Identification of the Corn Pathogen *Pantoea stewartii* by Mass Spectrometry of Whole-Cell Extracts and Its Detection with Novel PCR Primers. *Applied and Environmental Microbiology* 76(18): 6248–6256

Yadeta, K.A., and Tommas, B.P.H.J. 2013. The xylem as battleground for plant hosts and vascular wilt pathogens. *Frontiers in Plant Science* 4(97)

Yu, C. Wang, N., Wu, M., Tian, F., Chen, H., Yang, F., Yuan, X., Yang, C., and He, C. 2016. OxyR-regulated catalase CatB promotes the virulence in rice via detoxifying hydrogen peroxide in *Xanthomonas oryzae* pv. *Oryzae*. *BMC Microbiology* 16:269

Zhang, M., and Storz, G. 2000. Redox Sensing by Prokaryotic Transcription Factors. *Biochemical Pharmacology* 59: 1-6.

Zulperi, D., Manaf, N., Ismail, I., and S.K., Daljit. 2017. First report of *Pantoea stewartii* subspecies *stewartii* causing Fruit Bronzing of Jackfruit (Artocarpus heterophyllus), a New Emerging Disease in Peninsular Malaysia. *Plant Diseases* 101. 10.1094/PDIS-11-16-1689-PDN

Chapter II

A Membrane Localized RTX-Like Toxin Impacts Adhesion Properties and Hydrophobicity of the *Pantoea stewartii* Cell Envelope

Abstract

Characterized by the formation of water-soaked lesions and wilting of the plant, the causative agent of Stewart's Wilt, a severe disease of corn and maize is the phytopathogenic, gram negative bacterium *Pantoea stewartii* subspecies *stewartii*. Previously it has been shown that a large Repetitive Repeat-in-toxin or RTX-Like Protein, is the primary mediator of the formation of the water-soaked lesion symptom of this plant disease. Designated RTX2, this unique protein contains five putative Ca^{2+} binding domains, characteristic of RTX toxins. Despite its capability to facilitate the formation of water-soaked lesions, phylogenetic analysis indicates that this unique protein is more related to Biofilm Associated Proteins (BAP), a subfamily of RTX proteins, indicating the potential for additional functions. Through the use of molecular, microscopic and classical microbiology techniques and processes, our research group demonstrates that in addition to producing water-soaked lesions, RTX2 localizes to the bacterial cell envelope and influences the physiochemical properties of the bacterial cell envelope. This protein also impacts bacterial cell length, cell envelope integrity and overall cellular hydrophobicity. RTX2 influences adhesion and biofilm formation *in-vitro* and *in-planta*.

Introduction

Repeat-in-toxin (RTX) proteins have diverse roles in Gram negative bacteria. Functional examples of these proteins include proteases, lipases, adenylate cyclases and

cell surface S-layer proteins (Chang et al., 2014). Conserved features of RTX proteins include transport to the cell surface via the Type I secretion system (T1SS), a secretory signal often at the C-terminus, and glycine-aspartate (GD)-rich peptide repeats containing the consensus sequence G-G-X-G-(N/D)-D-X-(L/I/F)-X (X denotes any amino acid) for binding of calcium ions. Each repeat forms half of a portion of a ß-roll structure. A hydrophobic interior is formed by hydrophobic residues and each turn in the ß-roll structure contains a Ca^{2+} ion. These Ca^{2+} binding domains are vital for proper folding and activity of RTX toxins once these proteins are exported to the cell surface (Fiser and Konopasek, 2009; Chenal et al., 2010). Canonical RTX toxins include the 117 kDa, alpha (α) hemolysin from *Escherichia coli* (HlyA) and the adenylate cyclase toxin from *Bordetella pertussis* (Fiser and Konopasek, 2009). The latter toxin can damage bacterial membranes without using specific cellular receptors and forms small-cation selective membrane channels, flooding the interior of the host cell with monovalent cations, leading to osmotic lysis.

RTX toxins are also deployed by plant pathogens. The genome of *Pectobacterium atrosepticum* contains a coding sequence for a ~4600 amino acid long repeat containing protein with a C-terminal signal suggesting export via the Type I secretion system and homology to adhesins (Chang et al., 2014). RTX genes are also found in the genomes of *Xanthomonas oryzae* pv. *oryzae*, the causal agent of bacterial blight in rice, *Ralstonia solanacearum*, the causal agent of Southern wilt of tomato and *Xylella fastidiosa*, the causal agent of Pierce's Disease of grapevine and other diseases (Dossa et al., 2014; Salanoubat et al., 2002; Gambetta et al., 2018) but many of these are uncharacterized. In

addition to lytic activity, RTX proteins have diverse functions in bacterial infection. There are several subfamilies of RTX toxins and one is made up of large repetitive RTX adhesins, also collectively called biofilm associated proteins (BAP). BAPs often function as loosely attached adhesins and play a role in biofilm development (Satchell, 2011; Lasa and Penades, 2006).

In planta, *P. stewartii* colonizes both the leaf apoplast and the xylem of corn plants, causing leaf blight and wilt symptoms, respectively. During the leaf blight phase, the bacteria cause cellular damage that leads to accumulation of fluids in the surrounding leaf tissue that manifests as water-soaked lesions in young plants. In the xylem, the bacteria form robust biofilms encased in copious amounts of EPS that leads to xylem blockage and wilting of the plants. In *P. stewartii*, a RTX-like protein, designated RTX2, is responsible for water-soaked lesion formation in corn seedlings. While this 250 kDa protein shares similarities with other RTX toxins, it cannot be categorized into a specific subfamily of RTX proteins (Roper et al., 2015). Its orthologs include the large repetitive protein YeeJ in from *Pantoea ananatis*, and a putative hemagluttinin hemolysin adhesin–related protein from *Erwinia billingiae* (Roper et al., 2015). The *P. stewartii* RTX2 toxin contains five putative Ca^{2+} binding domains, a polycystic kidney disease (PKD) domain, five C-terminal transmembrane domains and an autotransport domain .Characteristic of RTX toxins, Ca^{2+} binding domains are vital for proper folding and activity of the toxin once exported to the cell surface, while the presence of transmembrane domain suggests it localized to the cell envelope.The presence of the autotransport domain suggests that unlike traditional RTX toxins, RTX2 is likely not be transported by Type I secretion like

other RTX proteins (Fiser and Konopasek, 2009; Chenal et al., 2010). The PKD domain is predicted to mediate interactions with other proteins and with carbohydrates (Roper et al., 2015; Ciccarelli, et al. 2002). In this study we determined that RTX2 is localized in the cell envelope of *P. stewartii* where it acts as a surface adhesion. Moreover, RTX2 contributes to overall cellular charge, cell surface hydrophobicity and cell length.

Materials and Methods

Bacterial Strains, Growth Conditions, and Strain Construction. All *P. stewartii* strains were grown on nutrient agar (Difco Laboratories, Detroit) at 28°C and *E. coli* strains were grown on LB at 37°C. Luria-Bertani (LB) broth (Difco Laboratories) was supplemented with 0.2% glucose (final concentration) where indicated. All pertinent strains of *P. stewartii* and *E. coli* are listed in Table 2.1. When needed and appropriate, the following antibiotics were added to microbiology media: nalidixic acid, 30 µg/ml; ampicillin, 100 µg/ml, kanamycin, 30 µg/ml, and tetracycline, 30 µg/ml (all final concentration). The *E. coli* S17-1λ strain served as a donor for conjugal transfer. The *Δrtx2/Δwceo* mutant was constructed using the method described for synthesis of the *Δrtx2* from Roper et al., 2015.

Electron Microscopy. Individual strains were inoculated into Luria Broth supplemented with 0.2% glucose and grown overnight at 28°C, at 180 rpm. Cultures were individually subcultured 1:20 into fresh media (of the same type) and allowed to grow until mid-log phase. Cells were harvested by centrifugation at 5000 rpm for 5 minutes, and washed with sterile PBS, pH 7.4. Cells were resuspended in sterile PBS, pH 7.4 and adjusted to

optical density (OD_{600}) of 0.3. Individual cell suspensions were then inoculated on onto separate acid washed glass-slides covered with sterile Poly-Lysine (Mfg: Cultrex, Catalog #3438-100-01) and allowed to sit for 30 minutes at 28°C. Samples were then taken to the UCR Central Facility for Advanced Microscopy and Microanalysis (CFAMM) for further processing and analysis. Prepared samples underwent critical point drying with a Tousimis 815 CriticalPoint Dryer and sputter coated. Samples were then viewed with a ThermoFisher Scientific (formerly FEI/Philips) NNS450 scanning electron microscope.

Quantification of Cellular Length and Width. Wild type and *Δrtx2* strains containing a plasmid constitutively expressing GFP (pHC60) were grown overnight in Luria Broth medium with 0.2% glucose (LBG) and 30 µg/ml tetracycline at 28°C with shaking at 180 rpm. Cultures were then diluted 1/20 in the same media type and allowed to grow at the same condition until mid-log phase was reached. One milliliter of each strain was individually spun down in a microcentrifuge, washed once and then resuspended in 150 µl of sterile Phosphate Buffered Saline (PBS) pH 7.4. Exactly 2 µl of each suspension was inoculated onto individual 2% agarose pads and imaged with a Confocal Inverted Zeiss 880 Airyscan UV PALM. Using a 40X water immersion lens, 3 randomly selected fields were taken for analysis with Imaris x64® software (version 9.1.2; Mfg.: Bitplane). From each field, ten cells were randomly selected and the length and width were measured. The entire experiment was repeated for a total of 3 biological replicates (with each biological replicate containing 3 fields containing each 10 cell measurements, for a total of 30 technical replicates for each biological replicate).

Quantification of Overall Cell Size. Single colonies of either wild type or *Δrtx2* were grown in LB medium with 0.2% glucose (LBG) overnight at 28°C with shaking at 180 rpm. Cultures were reinoculated into fresh LBG with 0.2% glucose at a final dilution of 1/20 and allowed to grow at the same conditions until mid-log phase was reached. Cells were then individually harvested by centrifugation (5000 rpm for 10 minutes). Cell pellets were washed and then resuspended to OD_{600} = 0.3 in sterile 10 mM KCl, pH 5.28. Particle size of cell suspensions were measured in a ZetaPal, zeta potential analyzer (Brookhaven Instruments Corporation, Holtsville, NY, U.S.A.). Results based on 3 biological replicates.

Localization of RTX2. Fractionation of bacterial cell envelope was prepared per Bennion et al., 2010 but with the following modifications: the complemented *rtx2* strain (*Δrtx2/rtx2*$^{+}$) from Roper et al, 2015, and its corresponding mutant (*Δrtx2* with the pBBR1-MCS4 vector) were grown, inverted at 28°C for 3 days on nutrient agar supplemented with nalidixic acid, 30 µg/ml. Cells were then harvested with sterile PBS, pH 7.4. Cells were pelleted by centrifugation at 5000 rpm for 10 minutes and stored at -80°C. Cells were then thawed on ice and resuspended at a concentration of 0.5 g/ml with Expedeon Proteoloc^{TM} EDTA-free Proteinase Inhibitor Cocktail. After lysozyme treatment for 30 minutes at 4°C, cellular suspension was lysed via French Press. Membrane and cytosolic fractions were separated by ultracentrifugation via 105,000 x gravity at 4°C for 60 minutes. Membrane (pellet) fraction was carefully resuspended in Tris Buffered Saline, pH 7.5, while the protein in the cytosolic (supernatant) fraction was precipitated via trichloroacetic acid precipitation and resuspended in SDS loading buffer.

For immunoblotting, the above samples were mixed with 2X Laemmli loading dye (Mfg. Biorad, Catalog 1610737), and boiled for 5 minutes. Samples were loaded onto a 4% stacking and 6% resolving SDS-PAGE gel and transferred onto a 0.2 µm Polyvinylidene fluoride (PVDF) membrane and blocked with 5% dried milk in Tris Buffered Saline, pH 7.4 with 0.1% Tween 20 (TBST). A rabbit polyclonal antibody raised against a synthetic peptide derived from RTX2 (SAELAFTVDNTGSSVALSPVG; both manufactured by Genscript) in TBST and 5% milk was used as the primary antibody (500 ng/ml, final concentration). Goat Anti-Rabbit IgG conjugated with Horseradish peroxidase (HRP; Mfg.: Agrisera, Cat# AS09 602) was used as the secondary antibody. The blot was developed with a Pierce^{TM} ECL Western Blotting Substrate, and read with a Biorad ChemiDoc XRS+.

Bacterial Adhesion to Hydrocarbon Assays. Single colonies of either wild type or *Δrtx2* were grown in LBG overnight at 28°C with shaking at 180 rpm. Cultures were subcultured into fresh LBG at a final dilution of 1:20 and allowed to grow at the same conditions until mid-log phase was reached. Cells were then individually harvested by centrifugation (5000 rpm for 10 minutes). Cell pellets were washed (by gentle inversion until solution is homogenous, without using a vortex) and then resuspended to OD_{600} = 0.3 in Phosphate Urea Magnesium Buffer (K_2HPO_4: 17 g, KH_2PO4: 7.26 g, Urea: 1.8 g, $MgSO_47H_2O$: 0.2 g), pH 7.1 (Tridbedi and Sil, 2014). Two milliliters of cell suspension were then aliquoted into sterile glass test tubes and OD_{600} was measured using a Thermo Scientific Biomate 3 spectrophotometer (Waltham, Massachusetts). This measurement served as the initial optical density reading (ODI). Then 2 ml of dodecane or n-

hexadecane was added to each separate tubes of cell suspension and vortexed for 2 minutes. After allowing the phases to separate for 2 hours, the second optical density reading (ODF) was taken. A control (no hydrocarbon added) for each culture was used to further monitor change(s) in optical density over time. The percentage of cell surface hydrophobicity of each strain was a modified version of the calculation from Tridbedi and Sil, 2014 and Swiatlo et al., 2002, calculated as follows: [(ODI-ODF)/ODI] x 100 of Treatment cells - [(ODI-ODF)/ODI] x 100 of control cells. Results are based on 4 biological replicates, each with 3 technical replicates.

Polymyxin B Challenges. For growth inhibition, single colonies of wild type, and *Δrtx2*, *P. stewartii* were grown overnight in LBG. The following day, cultures were diluted 1:20 and inoculated into fresh LBG in 96-well U-bottom microplates (Mfg. Falcon, Ref # 353077) to a final volume of 150 µl. Cells were treated with final concentrations of Polymyxin B (0 µg/ml (Negative Control), 6.25 µg/ml, 12.5 µg/ml, and 25 µg/ml). Growth was assessed in a Tecan Infinite F200 microplate reader using an absorbance reading of OD_{595} at room temperature. Measurements were taken every hour for 24 hours at room temperature, with 30 seconds of orbital shaking with an amplitude of 6 mm prior to each reading. Growth curve readings are based on 3 biological replicates, each containing 3 technical replicates. To evaluate overall survival, *Δrtx2* and wild type cells that were challenged with polymyxin B as described above were serially diluted with 1X phosphate buffered saline (PBS, pH7.4), plated onto nutrient agar with nalidixic acid (final concentration: 30 µg/ml), and incubated at 28°C for 2 days. The same concentrations of polymyxin B were used as for the growth curve (0, 25, 12.5, and 6.25

μg/ml). Percent survival was determined by dividing viable cell counts of antibiotic challenged bacteria by mock (negative control) viable cell counts. Results are based on 3 biological replicates, each containing 3 technical replicates.

SEM of *In Vivo* Biofilm Formation. Infection of 10-day old Jubilee Corn Seedlings was performed per Roper et al., 2015. At 5 days post inoculation, the entire corn plant was placed in a fixative solution containing 63% Ethanol with 5% glacial acetic acid and 5% formalin. Three-five 1 mm wide leaf strips were cut from the base part, middle portion, and tip portion of each leaf blade, respectively. The leaf strips were dehydrated through an ethanol series of 70%, 80%, 90%, 95%, 100% and 100% with 15 min at each step. Dehydrated leaf specimens were critical-point dried with Tousimis Autosamdsri-931 (Tousimis Research Corp., USA) and then sputter-coated with Au-Pd in a Safematic CCU-010 compact coating unit (Safematic GmbH, Switzerland). Coated specimens were examined and photographed under an SEM (Hitachi S3400-II) at the accelerating voltage of 8kV with a secondary electron detector.

Surface Adhesion Assays. Adhesion assays were based on Koutsoudis et al., 2006, Davies and Marques, 2009 and Theunissen et al. 2010. For preparation of etched assay plates: non-coated polystyrene plates (Mfg. Greiner Bio-One; Ref #655101) were exposed to acetone for 10 seconds. After removal of acetone, plates were inverted to allow evaporation of residual acetone. After sterilization by ultraviolet light for 1 hour, plates were further left open in a sterile, running biosafety cabinet overnight. For culture preparation: In brief, single colonies of wild type, *Δrtx2*, *Δwceo*, *Δwceo/Δrtx2* all carrying empty vector plasmid pBBR1, as well as *Δrtx2/rtx2*$^{+}$, and *Δwceo/Δrtx2/ rtx2*$^{+}$ were grown

at 28°C in LBG plus 100 µg/mL ampicillin with shaking at 180 rpm. After resuspending (by gentle inversion until solution is homogenous, without using a vortex) and centrifugation (5000 rpm for 10 minute) and washing twice in sterile PBS, pH7.4, these overnight cultures were all adjusted to OD_{600} = 0.5, then further diluted 1/10 in fresh LB broth supplemented with 0.2% glucose and 100 µg/mL ampicillin and inoculated into the acetone treated microplate to a final volume of 150 µl per well. One set of wells were incubated with only medium (with no antibiotics) to confirm proper sterilization of the plates. Cells were incubated statically at 28°C for 48 hours. After absorbance readings at OD_{595} in a Tecan Infinite M Plex microplate reader (Switzerland), planktonic cells and culture medium were removed and remaining surface-attached cells were adhered by incubation at 37°C for 60 minutes. Exactly 200 µl of a 1% crystal violet solution (dissolved in 95% ethanol, then filtered through a sterile 0.2-micron cellulose acetate filter housing) was then added to each well and the plates were incubated at room temperature, statically for an hour. The crystal violet solution was removed and each well was then washed three times with 200 µl sterile water with agitation for 30 seconds and dried overnight. The crystal violet was then solubilized by adding 200 µl of a 30% acetic acid solution per well, followed by a 1 hour shaking period on a Thermo Scientific MaxQ 2000 Orbital Shaker (Waltham, Massachusetts) set at 100 rpm at room temperature. The acetic acid solution from each well was further diluted 1 to 10 in 30% acetic acid in an untreated, polystyrene, 96-well microplate, mixed, and the absorbance reading were taken at OD_{595} in a Tecan Infinite M Plex microplate reader (Switzerland). The adhesion value or Specific Biofilm formation (SBF) was calculated as follows: (OD_{595}CV-media value)/

(OD_{595}Cell growth-media value; Niu and Gilbert, 2004). Results are based on 5 biological replicates, each containing 36 technical replicates (12 technical replicates from 3 separate, acetone treated microplates per biological replicate). Statistical analysis was performed using a linear mixed effects model, where adhesion value was the response variable, strain, biological replicate, and their nested interactions were fixed effects, and plate number and the interactions between plate and strain were random effects. Post hoc analysis was performed using the least-squares means method and was corrected for multiple comparisons using the "sidak" method. Statistical analysis was performed with R version 4.0.5 with Ime4 and emmeans packages.

Confocal Microscopy of *In-Vitro* Biofilms. Assays were based on Koutsoudis et al., 2006 with modifications. In brief, single colonies of wild type, *Δrtx2*, *Δwceo,* and *Δwceo/Δrtx2* all carrying plasmid pHC60, were grown separately overnight, at 28°C in LBG with 30 µg/mL tetracycline shaking at 180 rpm. After resuspending (by gentle inversion until solution is homogenous, without using a vortex), centrifugation (5000 rpm for 10 minutes) and washing twice in sterile PBS, pH7.4, these overnight cultures were all adjusted to OD_{600} = 0.5, then diluted further1/10 in fresh LB broth supplemented with 0.2% glucose and 30 µg/mL tetracycline. Then 7.5 ml of cell suspension was placed in a sterile 50 ml conical tube along with an autoclaved, confocal grade coverslip (Mfg.: Electron Microscopy Sciences, Cat # 72204-01). Prior to use, coverslips were gently etched with P220 grade sandpaper, rinsed with sterile water and sterilized by autoclave. Tubes were then incubated statically for 96 hours at 28°C. After gently rinsing the inoculated coverslip with sterile water, the biofilm formed at the location of the liquid air

interface was analyzed by placing the incubated coverslip on a glass slide covered with an adhesive microscope slide grid (Mfg: Diversified Biotech, Catalog # 89032-163), and viewed with a Zeiss 880 upright confocal microscope at 20X magnification. A total of 5 biological replicates were imaged with 11 images taken at individual grid points along the length of liquid air interface. BiofilmQ software developed by Hartmann et al., 2021 was used for quantitative three-dimensional image analysis of biofilms formed *in-vitro*. The Z-stack images analyses were based on Castro, 2021: formed biofilms were denoised by convolution using the default parameters, while floating cells were removed from images and a threshold of 100 vox was used to remove small artifacts due to noise. Top-hat filter was set to a value of 15 to remove background fluorescence. Images were segmented automatically with a sensitivity of 1.75, and use of the Otsu algorithm.

Autoaggregation Assays. Autoaggregation assays were based on Sorroche et al., 2012 with modifications. Individual strains were incubated overnight at 28°C at 180 rpm in Luria Broth supplemented with 0.2% glucose. After diluting 1/20 in 11.5 ml of fresh LB with 0.2% glucose, individual cultures were incubated under the same conditions until strains reached mid-log phase. Each culture was split into two, 5.5 ml volumes in separate sterile, 15 ml polypropylene tubes (Mfg.: Falcon, Ref # 352096) and both tubes were incubated at 4°C, for 18 hours. From the first tube: three, separate 0.1 ml aliquots were taken from just below the solution surface and were placed into individual wells of a 96-well polystyrene microplate (Mfg.: Greiner, Catalog # 655101) and read at an optical density of 595 nm (OD_{Final})The second tube, which served as a control was vortexed for 30 seconds, and three, separate 0.1 ml aliquots were placed into individual

wells of the same type of 96-well polystyrene microplate and also read at an optical density of 595 nm ($OD_{Initial}$). Sterile LB with 0.2% glucose served as a background control. After subtraction of background absorbance, the autoaggregation percentage was calculated as follows: 100 x [1 - ($OD_{final}/OD_{initial}$)]. Experiments were performed for a total of 5 biological replicates, each with 2 technical replicates. Statistical Analysis was performed using a Kruskal Wallis Test, followed by post-hoc Dunn's test.

Results

Deletion of *rtx2* Decreases Cell Length. Observations of *rtx2* mutant and wild type *P. stewartii* bacterial cells via scanning electron microscope observed differing dimensions between the two strains (Figure 2.2). Measurements of length and width by confocal microscopy showed the *Δrtx2* mutant to be shorter than the wild type (Figure 2.3). Both bacterial strains contain the plasmid pHC60 (which constitutively expresses GFP). Similar results were observed during particle size analysis by a ZetaPals, Zeta Potential Analyzer (Brookhaven Instruments). Wild Type *P. stewartii* also had a larger Average Diameter Eff. and half diameter when compared to the *Δrtx2* mutant (Figure 2.4).

RTX2 Localizes to the Cell Envelope. French press processing and further separation by ultracentrifugation yielded separate cell envelope (pellet) and cytosol (supernatant) fractions. SDS-PAGE followed by immunoblotting yielded distinct bands found only in the membrane fraction of *Δrtx2/rtx2*$^{+}$ (Roper et al., 2015). This strain expresses *rtx2* from a multicopy plasmid, allowing for increased expression of the protein compared with the

wild type. Immunoblot did not detect any such bands in the wild type cytosolic fraction, nor in either membrane or cytosolic fractions of the *rtx2* mutant with pBBR1 empty vector (Figure 2.5). The antibody also detected additional bands only in the membrane fraction of the overexpressing strain. This may be an artifact of the overproduction of RTX2, or perhaps the RTX2 protein is cleaved when it is in the cell envelope.

Deletion of *rtx2* Increases Sensitivity to Polymyxin B. RTX2 is predicted to be membrane bound and we hypothesize that the integration and membrane perturbation of the RTX2 protein in the cell envelope influences the physiochemical properties of the cell envelope. The antibiotic Polymyxin B destabilizes the bacterial outer membrane, by binding to the lipopolysaccharide layer (Hébrard et al., 2012), and can be used as an indication of membrane integrity. Deletion of *rtx2* increases sensitivity to Polymyxin B in all tested concentrations (25, 12.5 and 6.25 µg/ml), compared with the wild type (Figure 2.6A, 2.6B, and 2.6C).

RTX2 is Required for Colonization and Biofilm Establishment *In-Planta*. Scanning electron microscopy of 10 days old jubilee corn seedlings 5 days post inoculation yielded no visible bacteria in the lumen or xylem, while wild type *P. stewartii* was found heavily encased in EPS, in the xylem (Figure 2.7). Areas of highest bacterial concentration in the xylem corresponded to areas of water-soaked lesion development.

RTX2 Influences Cell Hydrophobicity and Surface Adhesion. Bacterial adherence to hydrocarbons (BATH) assays are a simple and rapid technique for determining cell surface hydrophobicity: change in optical density after mixing and exposure to an organic solvent is used to compare overall hydrophobicity of the cell surface (Rosenberg, 1984).

The more hydrophobic the cell, the more cells will be attracted to the organic phase, leading to a decrease in optical density measured in the buffer phase. BATH assays show that the *rtx2* mutant has higher adherence to the hydrocarbons dodecane or n-hexadecane (Figure 2.8).

In vitro crystal violet adhesion assays, demonstrated no significant difference in adhesion value (adhesion in proportion to bacterial growth measured by optical density) between wild type P. *stewartii* and the *Δrtx2* in an EPS-producing (wild type) background. However, *P. stewartii* produces high levels of EPS in culture, which can interfere with biofilm formation and surface adhesion in *in vitro* assays (Koutsoudis et al., 2006). The non-EPS producing (*Δwceo*) background mimics the initial stages of biofilm formation where bacteria attach to a surface, prior to the production of EPS (O'toole, 2003; Koutsoudis et al., 2006). In the non-EPS producing background (*Δwceo*), the deletion of *rtx2* (i.e., the *Δrtx2/Δwceo* double mutant) decreases the adhesion value when compared to the non-EPS producing wild type (*Δwceo* mutant). The *Δwceo* mutant also had a significantly higher adhesion value than all other strains, except the compliment strains. The complement strains in both EPS and non-EPS forming backgrounds showed a higher level of adhesion value than all other strains (Figure 2.9).

RTX2 Impacts Biofilm Height *In-Vitro* in a Non-EPS Background. Similar to the crystal violet adhesion results, only the wild type in the non-EPS background (*Δwceo*) showed a significant difference in biofilm height, when compared to all the other strains. The *wceo* mutant (non-EPS producing wild type) was significantly taller than the other

strains (Figure 2.10). Results are based on 5 biological replicates, each with 11 technical replicates.

RTX2 has no Impact in Cell to Cell Aggregation *In-Vitro*. Autoaggregation Assays indicated that RTX2 appears to have no influence in cell-cell aggregation, i*n-vitro* (Figure 2.13). The only significant difference was seen in the wild type strain in an EPS producing background. However, this difference was a decrease in the percentage of autoaggregation. The *rtx2* mutant, in its non-EPS producing counterpart (*Δrtx2/Δwceo*), and even the non-EPS producing wild type (*Δwceo*) showed no significant difference in autoaggregation.

Table 2.1. Bacterial Strains and Plasmids

Strain or Plasmid	Relevant Genotypes	Source
Pantoea stewartii subsp. *Stewartii*		
DC283	Wild type, NaI^r	Coplin et al. 1986
Δrtx2 (CR54)	NaI^r, knockout in *rtx2*	Roper et al., 2015
Δwceo	NaI^r, knockout in *wceo*	Carlier et al, 2009
Δrtx2/ Δwceo (CR59)	NaI^r, knockout in *wceo / rtx2*	This study
Δrtx2/rtx2$^+$ (CR64)	*Δrtx2*, pMCR29. parent strain DC283	Roper et al., 2015
DC283 w/ pBBR1 (EV)	NaI^R, Ap^R	This study
Δrtx2 w/ pBBR1(EV)	*Δrtx2*, NaI^R, Ap^R	This study
Δwceo w/ pBBR1(EV)	*Δwceo,* NaI^R, Ap^R	This study
Δrtx2/ Δwceo w/ pBBR1(EV)	*Δrtx2/ Δwceo,* NaI^R, Ap^R, Kan^R	This study
Δrtx2/ Δwceo/ rtx2$^+$	*Δrtx2/ Δwceo,* NaI^R, Ap^R, Kan^R pMCR29. parent strain DC283	This study
Escherichia coli		
S17-1λ	RP4, Mob+, Smr	Simon et al. 1983
Plasmids		
pHC60	Broad host range vector carrying *gfp*, tet^R	Cheng & Walker, 1998
pMCR29	*rtx2* cloned into pBBR1	Roper et al, 2015
pBBR1-MCS4	Broad host range vector, Ap^R	Kovach, et al. 1995

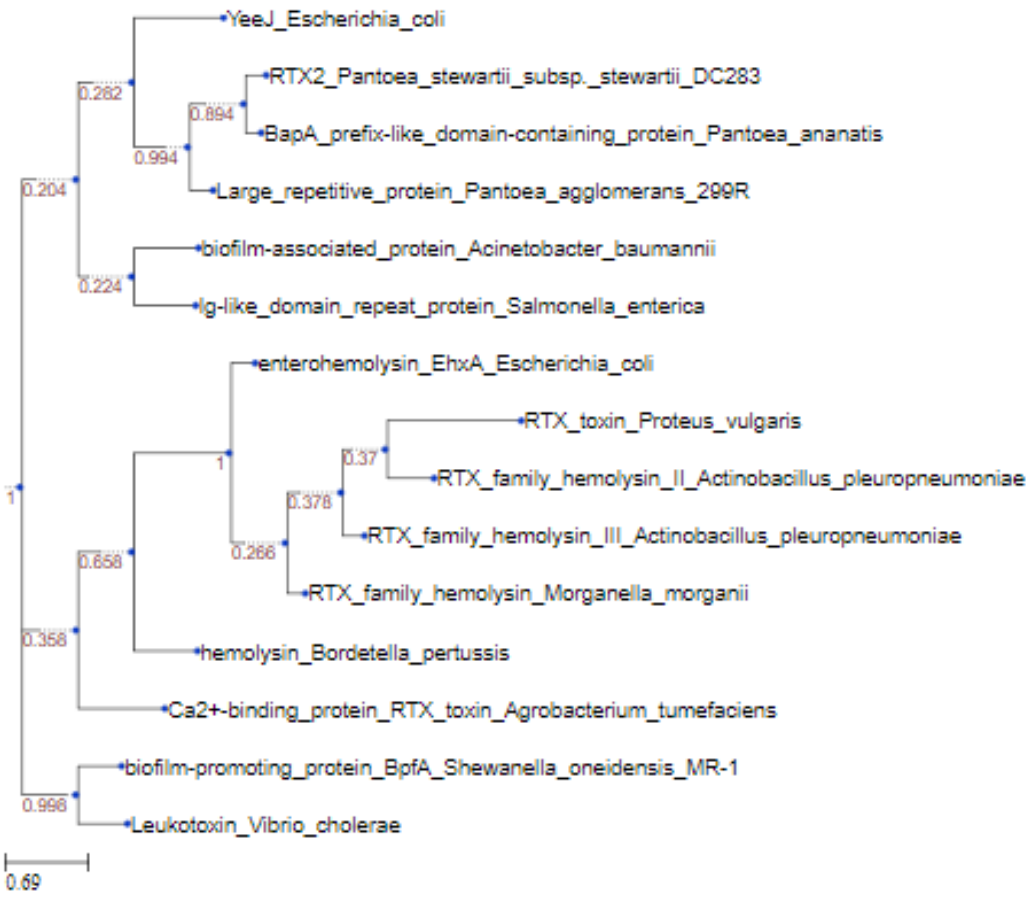

Figure 2.1. Phylogenic Tree relating Domain Relationship of RTX2 to other similar proteins. Using TREND software from Gumerov, and Zhulin, 2020 a phylogenic tree based on protein domains was determined. The protein RTX2 appears to be more related to Biofilm associated proteins than traditional RTX toxins.

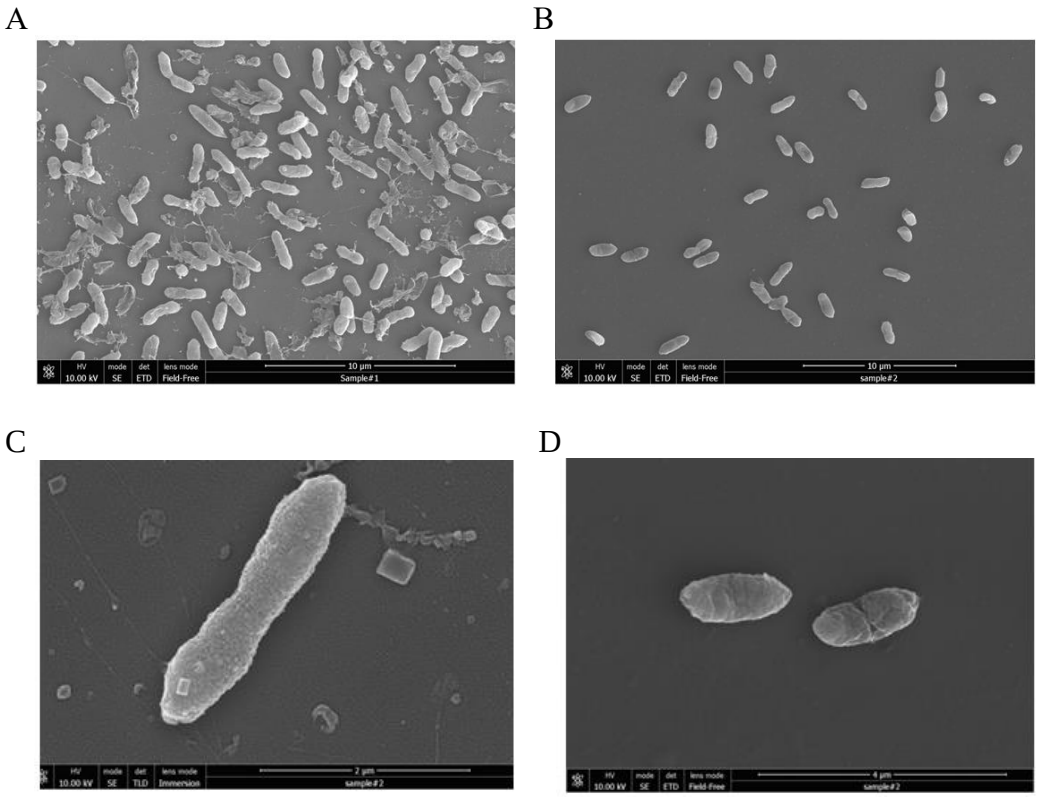

Figure 2.2 The *Δrtx2* mutant cells are shorter in length as compared to wild type *Pantoea stewartii*. Scanning electron microscopy shows the wild type *P. stewartii* (A and C) to be longer than the *rtx2* mutant (B and D). Scanning electron Microscopy Images were performed on a NNS450 Scanning Electron Microscope. All bacterial electron microscope work was done at Central Facility for Advanced Microscopy and Microanalysis (CFAMM) facility at UCR.

A

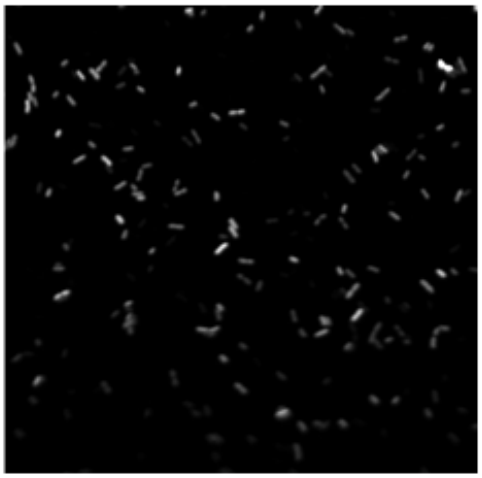

B

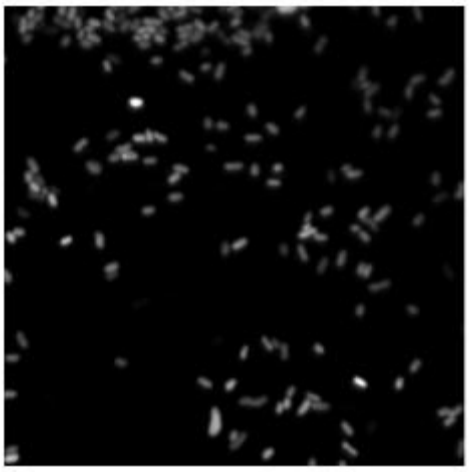

C

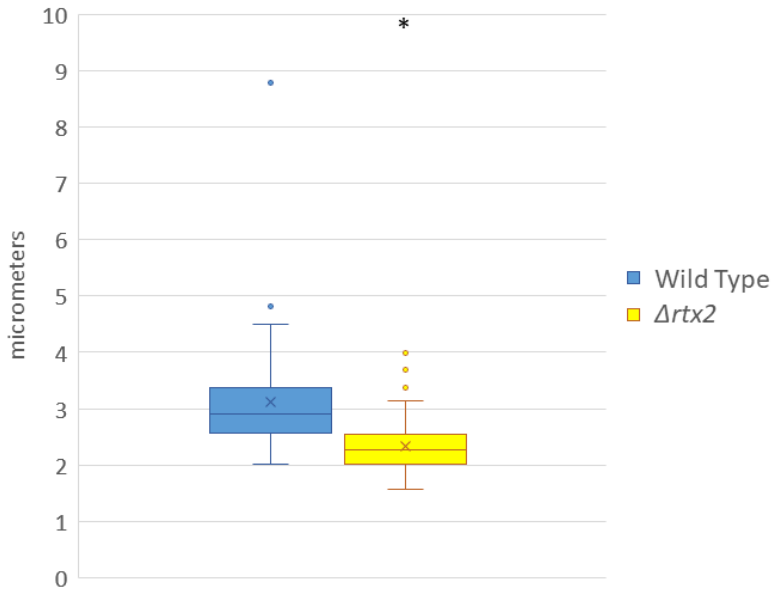

Figure 2.3. Deletion of *rtx2* decreases length of the bacterial cell. Confocal images of A) wild type and B) *Δrtx2*. The length of individual wild type and *Δrtx2* strains containing the plasmid pHC60 (which constitutively expresses GFP) were measured by a Confocal Inverted Zeiss 880 Airyscan UV PALM Imaris x64® software (version 9.1.2; Mfg.: Bitplane; C). * indicate treatments that are statistically different at $p \leq 0.05$ by t-test. Results are based on 3 biological replicates, each with 30 technical replicates.

A

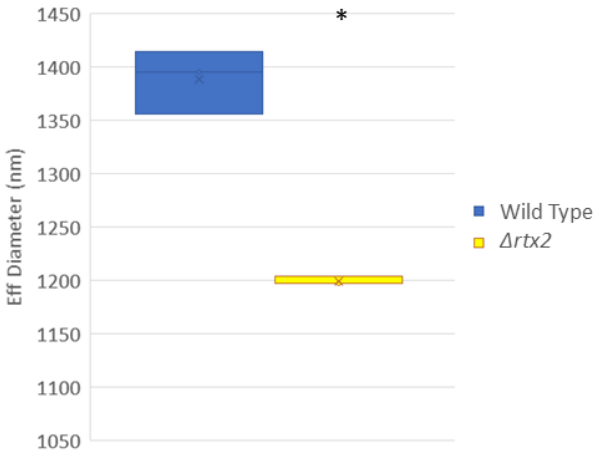

B

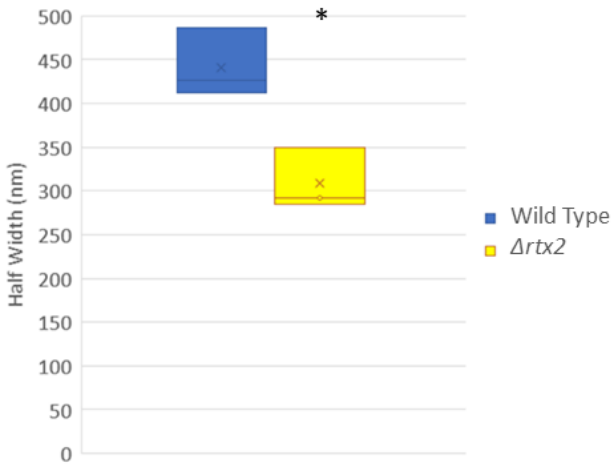

Figure 2.4. Particle Size Analysis of wild type versus *Δrtx2* show that wild type *P. stewartii* is larger. Wild Type *P. stewartii* shows A) larger Average Diameter (Eff. Diameter), * indicates p = 0.0004 by t-test and B) Half Diameter (half the width measured at half the height) when compared to *Δrtx2* mutant. * indicated p = 0.0123 by t-test. Results are based on 3 biological replicates.

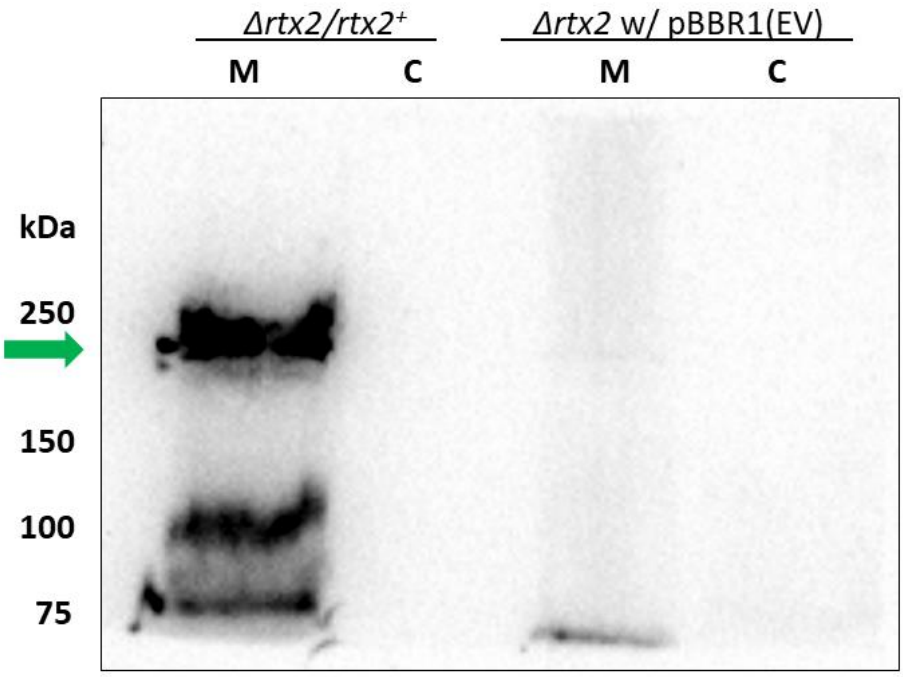

Figure 2.5. RTX2 is detected in membrane fraction of the cell. Rabbit polyclonal antibody raised against a peptide (SAELAFTVDNTGSSVALSPVG) designed from a portion of the RTX2 protein (Genscript) detected a protein of approximate size to RTX2 in the membrane fraction (indicated with a green arrow) of the complimentary strain of *rtx2* mutant *P. stewartii (*Δ*rtx2/rtx2*$^{+}$) and not in the cytoplasmic fraction of the same strain of bacteria, and neither in the membrane or cytoplasmic fractions of the corresponding *rtx2* mutant *(*Δ*rtx2* w/ pBBR1 (EV; Empty vector). Equal amounts (1 µg) of membrane or cytoplasmic fractions of either the overexpressing strain of wild type or *Δrtx2 P. stewartii* were run on a 4% stacking / 6% resolving sodium dodecyl sulfate (SDS) Denaturing Gel and transferred onto 0.25 µM Polyvinylidene fluoride membrane. Goat anti-Rabbit IgG conjugated with horseradish peroxidase (HRP) was used for detection.

.

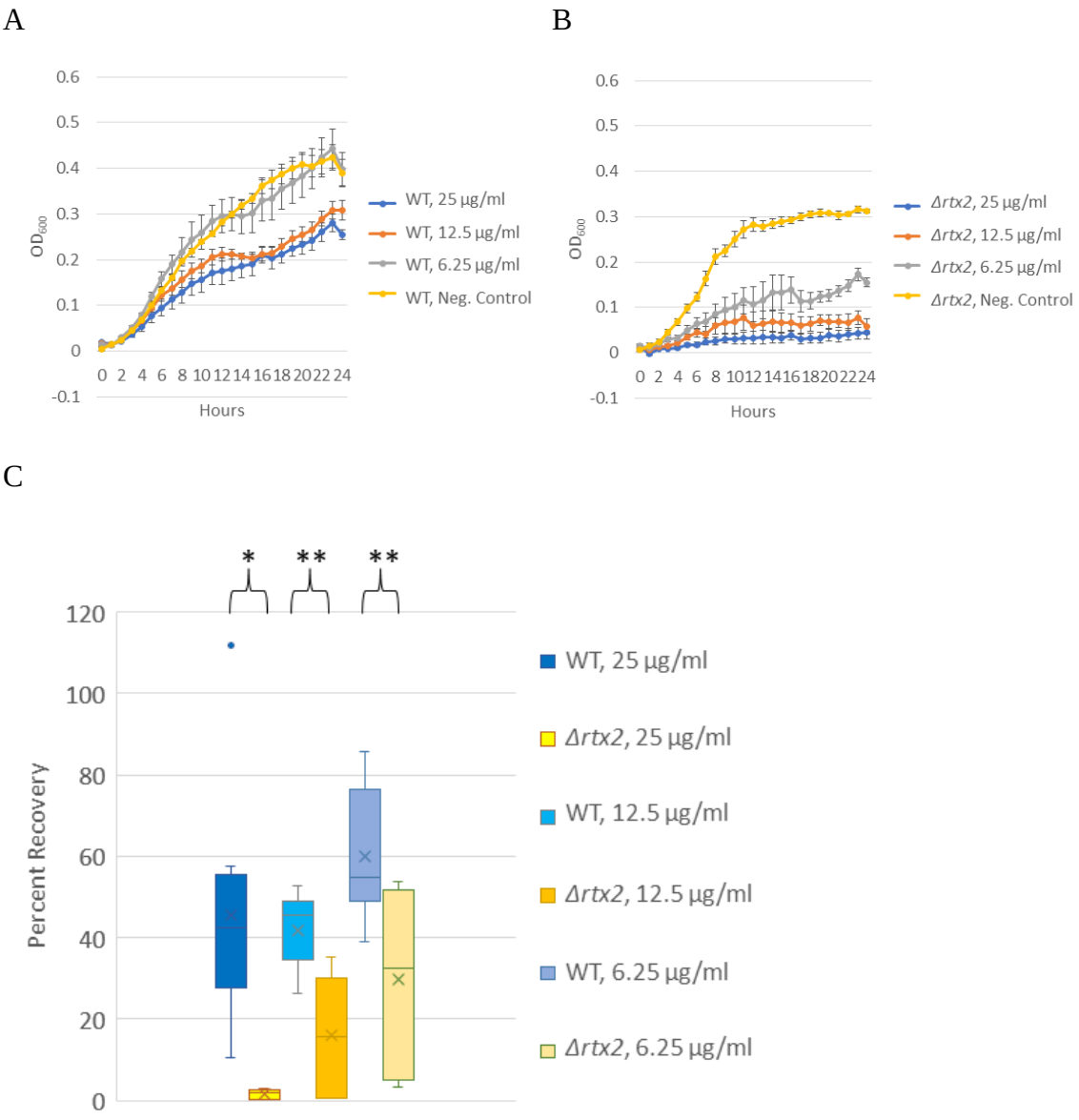

Figure 2.6. **Deletion of *rtx2* impacts resistance to Polymyxin B.** Growth curve experiments with both A) wild type and B) *Δrtx2* strains were incubated statically overnight against varying concentrations of the cell envelope targeting antibiotic Polymyxin B. Error Bars denote standard error. End Point plate counts C) showed the *Δrtx2* mutant with increased sensitivity to Polymyxin B versus the wild type. * indicates treatments that are statistically different at $p \leq 0.002$, while ** $p \leq 0.0001$ by t-test. Experimental Results are based on 3 biological replicates, each with 3 technical replicates.

A.

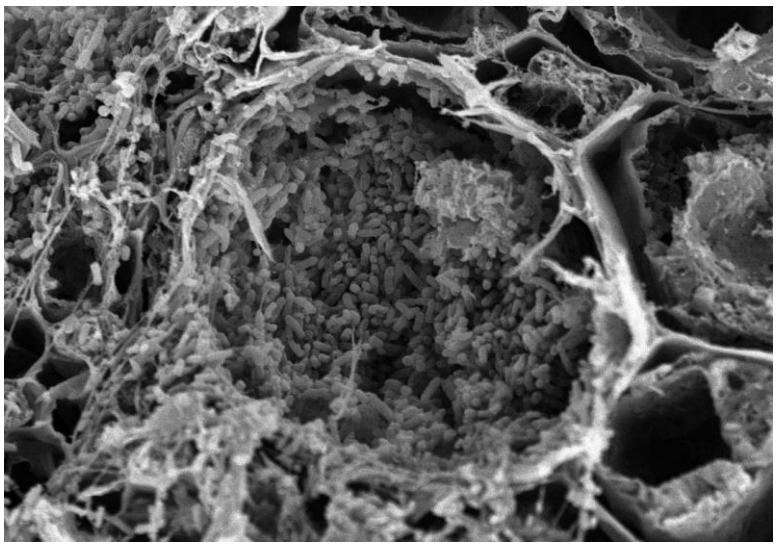

B.

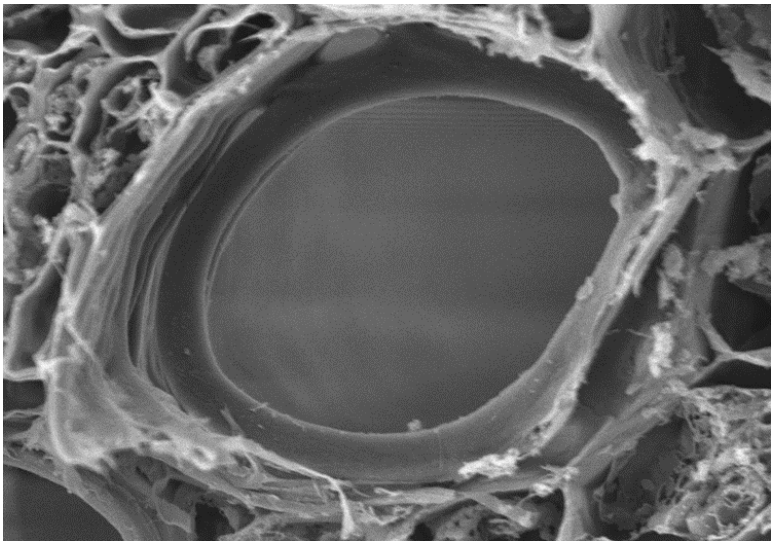

Figure 2.7. RTX2 is required for biofilm formation *in-planta*. Representative SEM Images of A) wild type *P. stewartii* and B) *Δrtx2* inoculated plants showed that the RTX2 protein is needed by the bacteria to form the EPS-based biofilm characteristic of Stewart's wilt. SEM images of inoculated plants, 5 days post infection show that while wild type *P. stewartii* is found in the xylem, the *rtx2* mutant is not present in significant numbers to be detected.

A

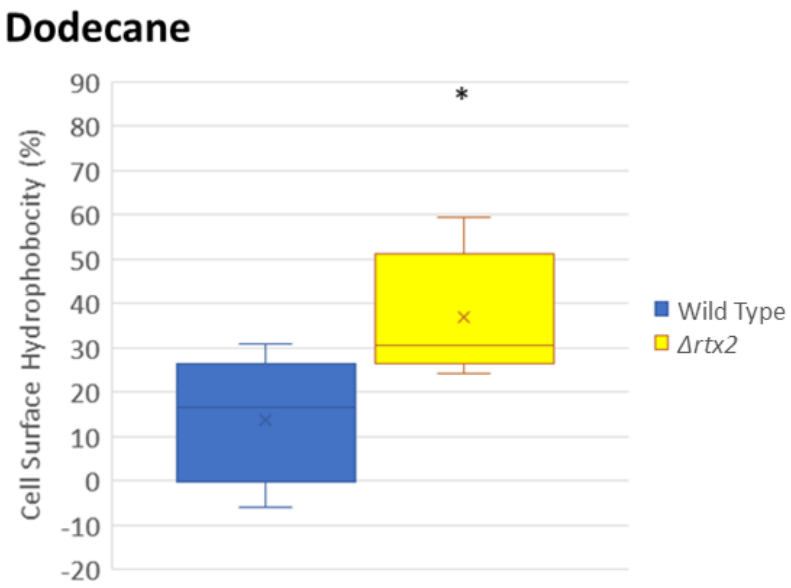
Dodecane
Cell Surface Hydrophobocity (%)
90
80
70
60
50
40
30
20
10
0
-10
-20
*
Wild Type
Δrtx2

B

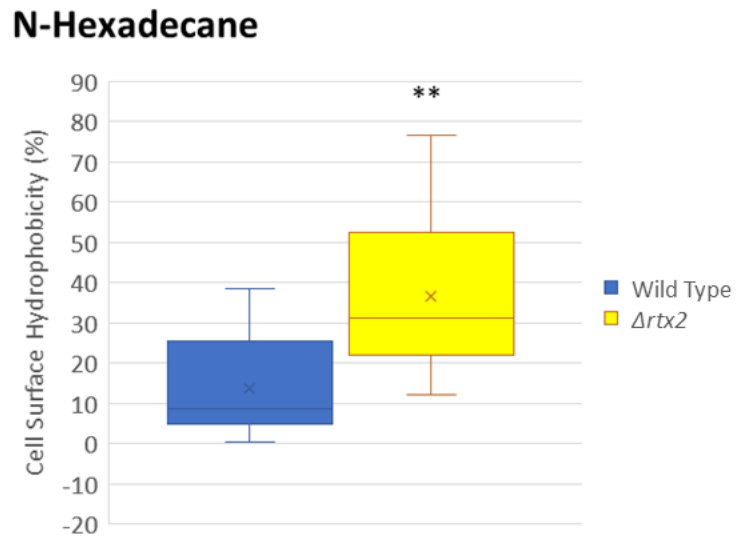
N-Hexadecane
Cell Surface Hydrophobicity (%)
90
80
70
60
50
40
30
20
10
0
-10
-20
**
Wild Type
Δrtx2

Figure 2.8. **Deletion of *rtx2* increases cell surface hydrophobicity.** Bacterial Adhesion to Hydrocarbon (BATH) Assays using the organic solvent A) Dodecane or B) N-Hexadecane indicates that the *rtx2* mutant has increased cell surface hydrophobicity compared to the wild type. * indicates significance at $p < 0.0001$ and ** $p < 0.002$ via Mann Whitney Test. Results are based on 4 biological replicates, each with 3 technical replicates.

A

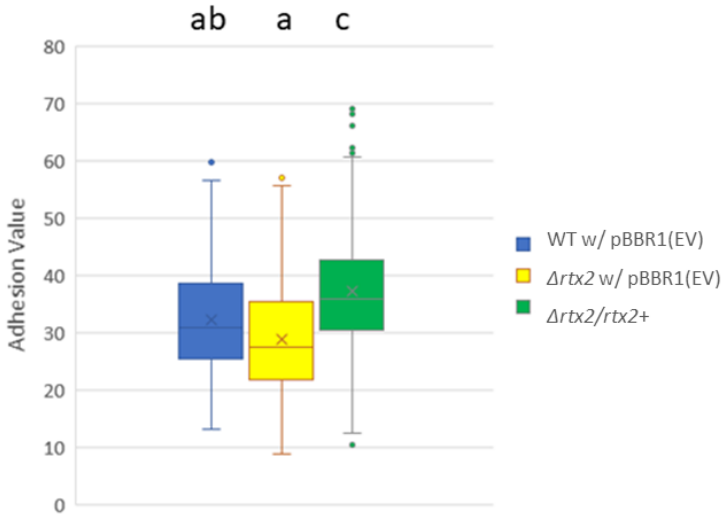
ab
a
c
Adhesion Value
80
70
60
50
40
30
20
10
0
WT w/ pBBR1(EV)
Δrtx2 w/ pBBR1(EV)
Δrtx2/rtx2+

B

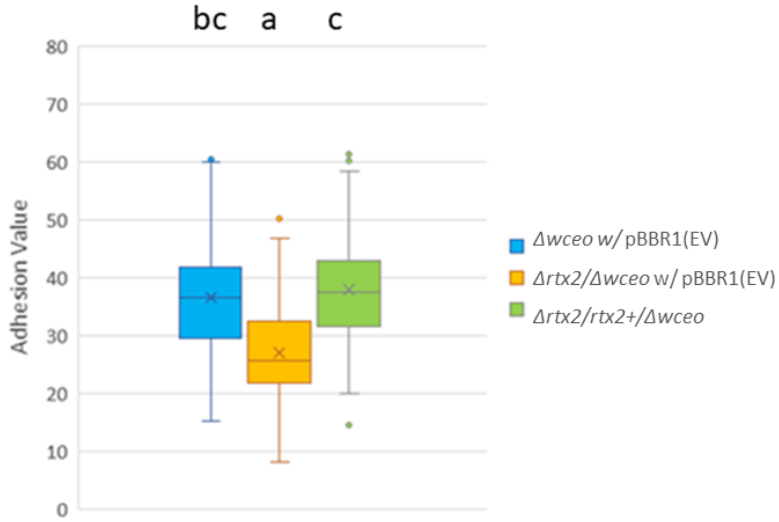
bc
a
c
Adhesion Value
80
70
60
50
40
30
20
10
0
Δwceo w/ pBBR1(EV)
Δrtx2/Δwceo w/ pBBR1(EV)
Δrtx2/rtx2+/Δwceo

Figure 2.9. **Deletion of *rtx2* decreases surface adhesion *in-vitro*.** Surface Adhesion Crystal Violet Assays with acetone treated, uncoated microplates showed A) no major difference in adhesion value (adhesion in proportion to bacterial growth measured by optical density) between wild type *P. stewartii* and the *Δrtx2* in an EPS-producing background. B) In a non-EPS producing (*Δwceo*) background, the deletion of *rtx2* (i.e., *Δrtx2/Δwceo* mutant) decreases the adhesion value when compared to the non-EPS producing wild type (*Δwceo* mutant). In the *Δwceo* (non-EPS producing) background, the wild type (*Δwceo* mutant) had a significantly higher adhesion value versus the EPS producing wild type, *Δrtx2*, and the non-EPS producing *Δrtx2/ Δwceo*, suggesting a role of the RTX2 protein as an adhesin. The complimenting strains in both EPS and non-EPS forming backgrounds showing a higher level of adhesion value than all other strains. Adhesion value or Specific Biofilm formation (SBF) was calculated as follows: (OD595CV-media value)/(OD595Cell growth-media value)(Niu and Gilbert, 2004). Statistical analysis was performed using a linear mixed effects model, followed by a post hoc analysis using the least-squares means method with the "sidak" method to correct for multiple pairwise comparisons. Letters denote levels of significance.

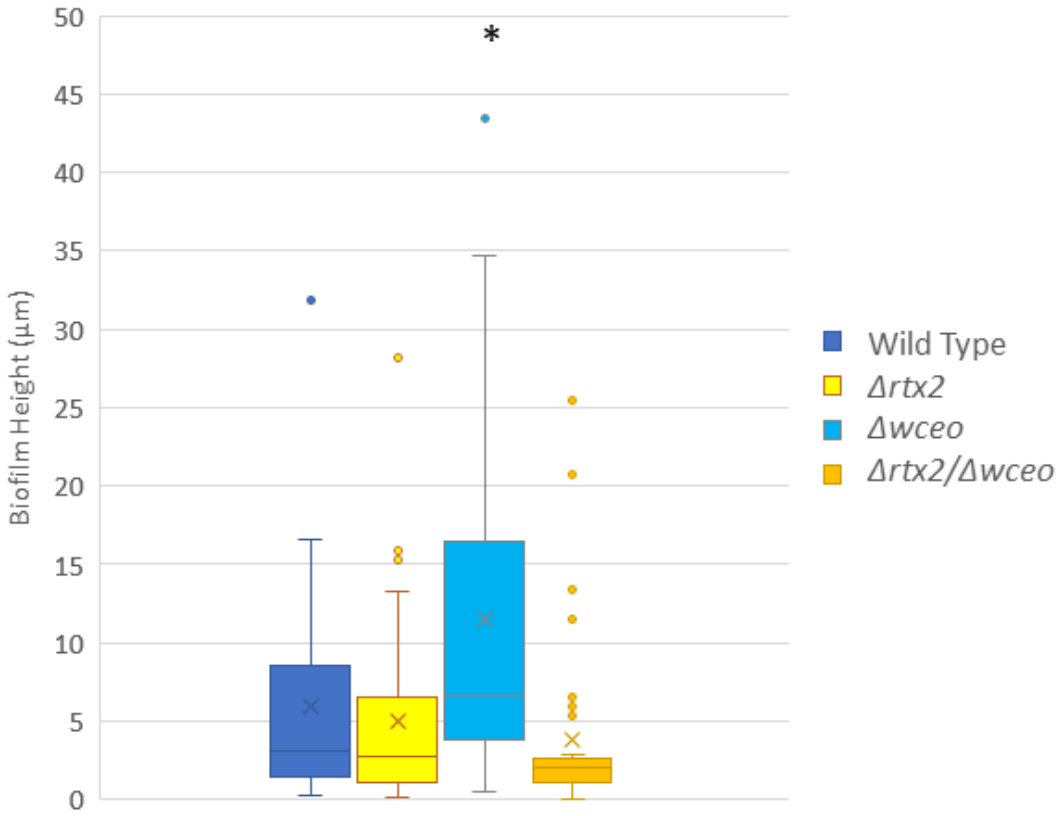

Figure 2.10. Deletion of *rtx2* decreases height of biofilms (*in-vitro*). Analysis of 3-D, confocal imaging of the above strains of *P. stewartii* by BiofilmQ (Hartmann et al., 2021) show deletion of *rtx2* leads to a decrease in height, in a non-EPS forming background. Results are based on 5 biological replicates, each with 11 technical replicates. * indicates significance at $p < 0.01$ via ANOVA plus post hoc Tukey HSD test.

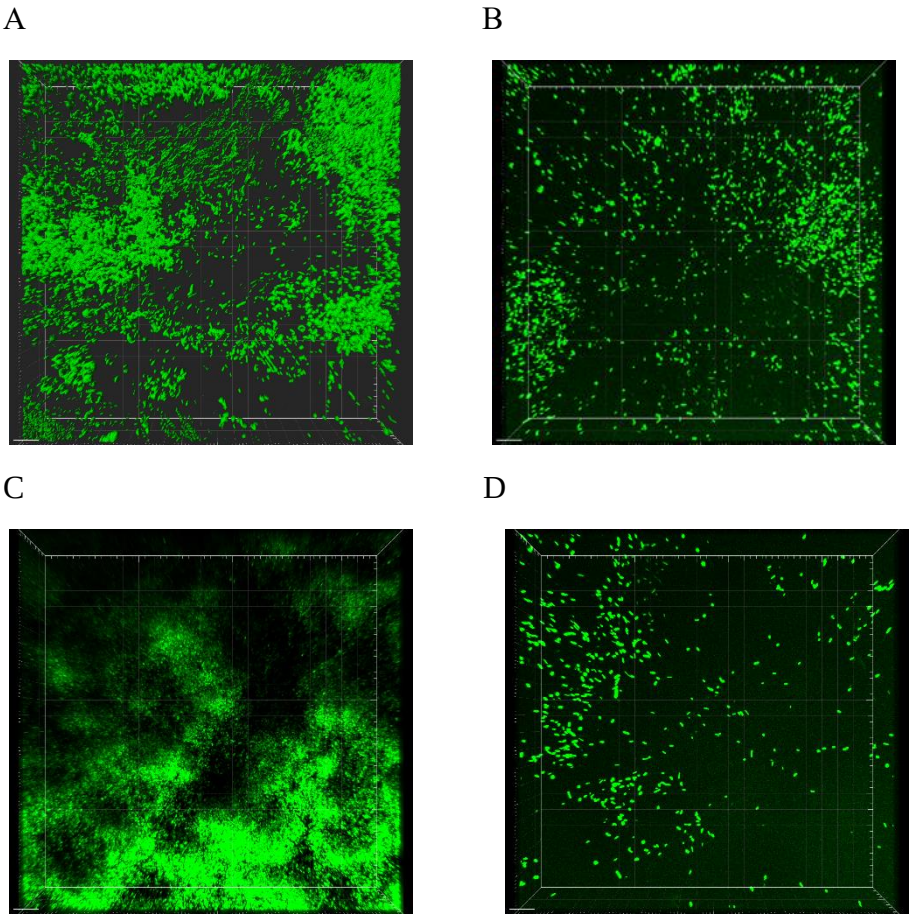

Figure 2.11. Observed impact of the deletion of *rtx2*. Deletion of *rtx2* impacts biofilm formation (*in-vitro*). Representative Imaging of GFP tagged A) Wild Type B) *Δrtx2* C) *Δwceo* and D) *Δrtx2/Δwceo* expressing plasmid pHC60, allowing for constitutively GFP expressing shows increased observed biofilm formation in wild type and *Δwceo* strains.

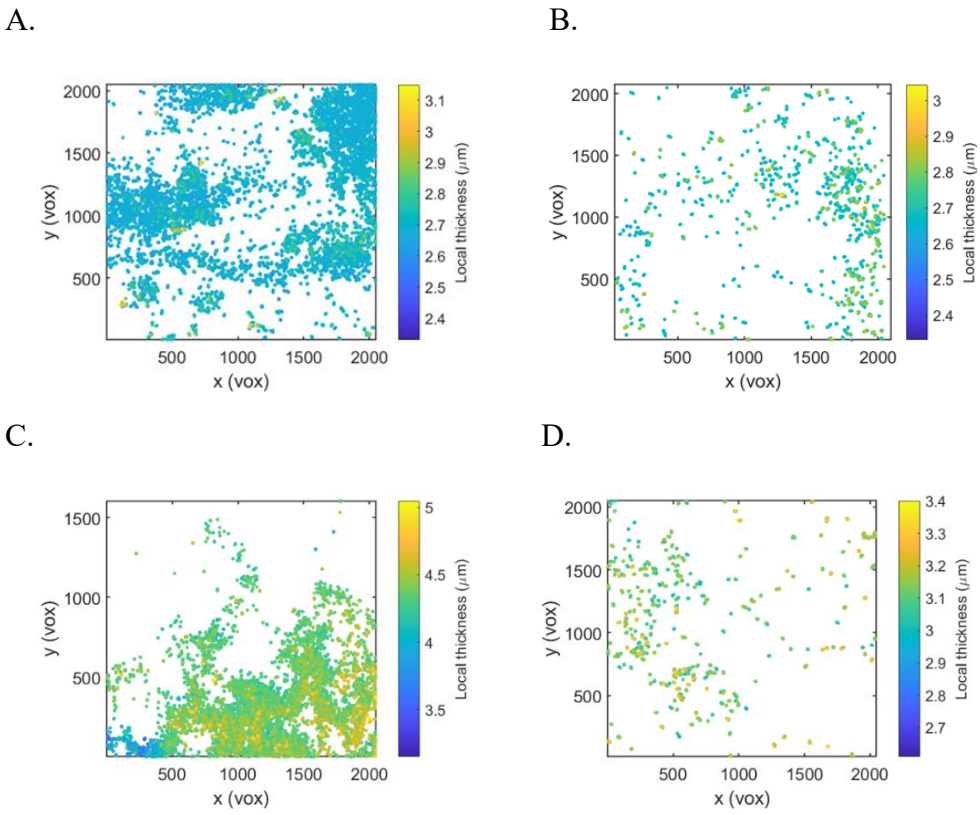

Figure 2.12. Determined Thickness of representative images of GFP tagged bacteria. A) Wild Type B) *Δrtx2* C) *Δwceo* and D) *Δrtx2/Δwceo* strains of *P. stewartii* expressing plasmid pHC60 from Figure 11. Calculation of Local thickness of the representative images and resulting figure is by BiofilmQ (Hartmann et al., 2021) shows the *wceo* mutant to be taller than all other strains.

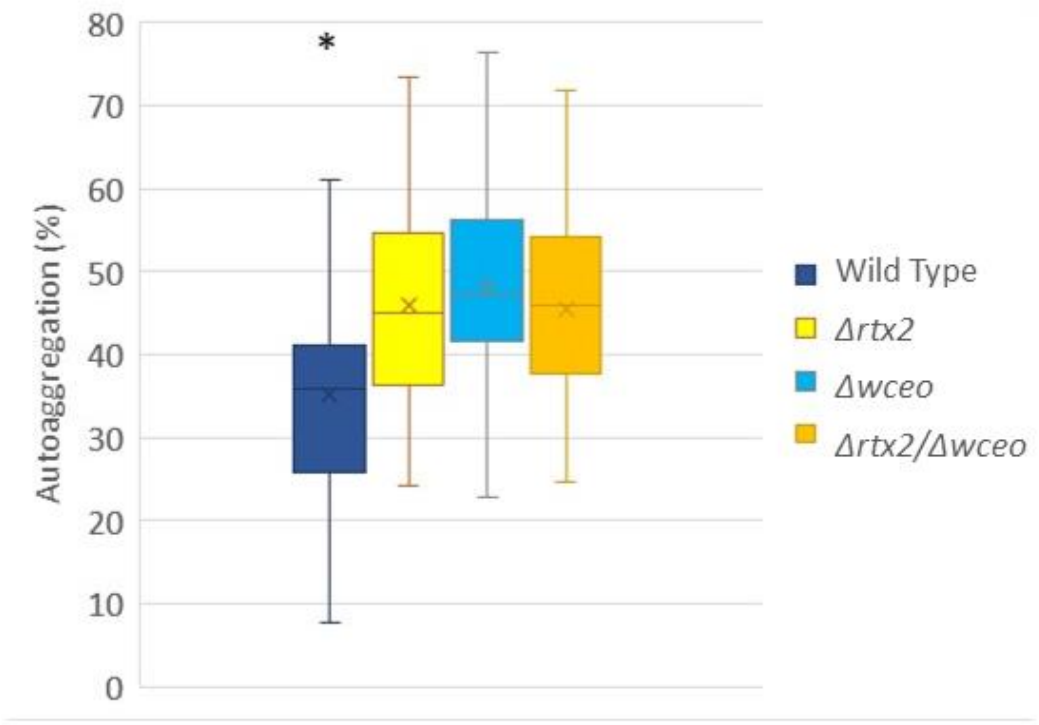

Figure 2.13. RTX2 has no impact on cell to cell autoaggregation, *in-vitro*. Autoaggregation Assays showed that only the EPS-producing wild type *P. stewartii* had a significant difference, but it resulted in a decrease in autoaggregation. Results are a total of 5 biological replicates, each with 2 technical replicates. Statistical Analysis was performed using a Kruskal Wallis Test, followed by post-hoc Dunn's test, with $p \leq 0.005$.

Discussion

Bap-like RTX proteins are implicated in biofilm formation several bacterial systems such as *Pseudomonas fluorescens, Escherichia coli, Acinetobacter baumanii,* and *Staphylococcus aureus* among others where they are required for the formation of 3-dimensional tower structures and biofilm maturation (Lasa and Penades, 2006; Brossard and Campagnari, 2011). In addition to to having cytolytic activity, the *P. stewartii* RTX2 also has large repetitive adhesin motifs homologous to hemagglutinins and to the Bap subfamily of RTX proteins suggesting it plays a pleiotropic role as an adhesin and a cytolysin (Roper et al., 2015, Tao et al., 2006, Heidelberg et al., 2004). Comprehensive images of biofilms formed on glass slides indicated that the 3-dimensional biofilm morphologies were, indeed, qualitatively different than the isogenic wild type strain. Specifically, the wild type cells readily colonized the glass surface and formed congruent biofilms, whereas, the *Δrtx2* mutant sparsely populated the glass slides resulting in a patchy biofilm. Although the domain architecture of RTX2 suggested it behaves as an adhesin, the *Δrtx2* mutant was similar to the wild type parent when assayed for direct cell-to-surface adhesion properties to polystyrene using a crystal violet assay designed to isolate the initial attachment to a surface. This suggested that RTX2 may play a nuanced role in adhesion that affects fine-scale downstream biofilm architecture but is not apparent during initial surface attachment or cell-cell adhesion in traditional crystal violet assays.

In canonical biofilm development, biofilm initiation is mediated by cell surface adhesins that allow for attachment to surface substrata and cell-cell aggregation that lead

to microcolony formation. Once established in a microcolony, the biofilm cells differentiate and begin producing an extracellular matrix that contributes to the building and maintenance of the biofilm architecture (O'toole, 2003). *P. stewartii* produces copious amounts of EPS called stewartan that is necessary for biofilm maturation. Stewartan forms a very fluid, slime layer that is loosely associated with the cell surface and can often mask nuanced roles of surface adhesins by preventing strong adherence to the surface substrata (Koutsoudis et al., 2006). Because *P. stewartii* does not strongly adhere to surfaces due to its fluid EPS, we tested the role of RTX2 as adhesin in absence of the confounding effects of stewartan EPS by introducing the *rtx2* mutation into the *Δwceo* genetic background that is defective in EPS production. WceO is a glucosyl-transferase involved in EPS production in *P. stewartii* (Carlier et al., 2009). Indeed, the *Δrtx2/Δwceo* was significantly impaired in attachment to the polystyrene substrate indicating that RTX2 has adhesive properties.

However, even in a non-EPS producing ($\Delta wceo$) background, RTX2 does not appear to play a role in cell to cell aggregation. There was no significant difference between the non-EPS producing wild type ($\Delta wceo$) and the non-EPS producing *rtx2* mutant ($\Delta rtx2/\Delta wceo$). While the wild type (EPS-producing) *P. stewartii* was the only strain to show any significant difference, it was in a decrease in autoaggregation. This could be due to the *in-vitro* characteristics of wild type *P. stewartii* producing excess EPS, which may prevent cell to cell interaction (Koutsoudis, et al., 2006). This phenomenon also may impact the *in-vitro* biofilm height, as seen in the confocal based visualization of the wild type (EPS-producing), GFP-tagged bacteria.

In planta, *P. stewartii* colonizes both the leaf apoplast and the xylem, causing leaf blight and wilt symptoms, respectively. During the leaf blight phase, the bacteria cause cellular damage that leads to accumulation of fluids in the surrounding leaf tissue that manifests as water-soaked lesions. In the xylem, the bacteria form robust biofilms encased in copious amounts of EPS that leads to xylem blockage and wilting of the plants. Both the leaf apoplast and the xylem present a mosaic of hydrophilic and hydrophobic surfaces that the bacterium must adhere to during the infection process. Thus, *P. stewartii's* ability to change its surface properties during the interaction with different tissue niches in the plant is critical to the infection process. Cell surface hydrophobicity is a multifactorial phenotype dictated by the composition of the bacterial cell surface and is an important parameter that governs bacterial attachment and detachment to biotic surfaces. Hydrophobicity can be impacted by cell envelope structures including lipopolysaccharides and cell surface proteins (Lahesaare et al., 2016). Microorganisms can fine tune their cell surface hydrophobicity in response to changes in environmental conditions (temperature, composition of nutrients, etc.) and growth phases (Heipieper et al., 2010) that, in turn, affects their adhesion to surfaces. Surface localized adhesins, such as LapF, from *Pseudomonas putida* and YcfR of *E. coli* contribute to overall cell surface hydrophobicity (Zhang et al., 2007; Lahesaare et al., 2016). The Bap-like protein, Esp, from biofilm forming strains of *Enterococcus faecalis* promotes primary attachment to surfaces and also is an important contributor to cell surface hydrophobicity (Toledo-Arana, et al., 2001). Membrane fractionation and immunoblot experiments confirmed that the RTX2 protein localized to the *P. stewartii*

envelope as predicted by the five transmembrane domains in the C-terminus. Moreover, deleting *rtx2* resulted in a significant increase in cell surface hydrophobicity of *P. stewartii* indicating either that the RTX2 protein imparts hydrophilic properties to the cell surface or that deleting RTX2 exposes hydrophobic entities on the cell surface. Based on this, we speculate that RTX2 plays a role in early attachment where it acts as a primary adhesin by modulating cell surface hydrophobicity. Both the apoplastic phase and xylem colonization phases require attachment to host surfaces. RTX2 is implicated in water-soaked lesion formation where it causes cellular damage that leads to accumulation of fluids in the surrounding leaf tissue that manifests as water-soaked lesions. In tandem with RTX2, a Type III effector, WtsE, is also required for water-soaked lesion formation (Roper et al, 2015; Ham et al., 2006) The Type III secretion system functions by directly injecting effectors into host cells and, thus, requires host cell contact. We speculate that RTX2 is an important contributor to host cell attachment particularly during the apoplastic phase of colonization to enable its own access to the plant cell as well as facilitating the host cell contact required for delivery of the WtsE effector.

Determination of cell size is a multi-faceted and complex process and the mechanisms that govern cell size can diverge substantially among bacterial species. Spatiotemporal mathematical models of biofilm assembly predict that cell length has an impact on shaping biofilm structure. Specifically, a longer average cell length yields more rapidly expanding, flatter biofilms than those formed by shorter cells (Beroz et al., 2018). Deletion of *rtx2* resulted in a significant reduction in bacterial cell size when compared to wild type *P. stewartii*. We speculate that its role in modulating cell size also

is a factor in its role in biofilm formation. It is unknown how this surface localized protein aids in determination of cell size or why a smaller cell size impacts biofilm development. However, the *rtx2* gene is found in an operon with two components of the Regulator of Capsular Synthesis (Rcs) phosphorelay regulatory system, the phosphotransferase RcsD, and the response regulator, RcsB (Burbank, 2014). The Rcs phosphorelay is an environmental responsive, multi-component signal transduction system that regulates EPS production, cell division, integrity of the cell envelope, biofilm formation, flagellar genes and virulence factors (Hinchliffe et al., 2008). Because RTX2 localized to the cell envelope and *rtx2* may be co-transcribed with *rcsB* and *rcsD* (see Chapter 3) , we hypothesize RTX2 may also be linked to fine-tuning of the physiochemical properties of the bacterial cell that are linked to the Rcs phosphorelay.

Establishment and synthesis of a biofilm is a complex, coordinated endeavor. In this study we determined that the *P. stewartii* Bap-like RTX2 affects the physiochemical properties of the cell envelope, and mediates cell surface attachment in addition to its previously determined cytolytic role in water-soaked lesion formation (Roper et al, 2015). However, despite the activity of the multifunctional protein RTX2, more research is required to determine all related protein activity during the biofilm process, as *P. stewartii* forms a biofilm as part of infection cycle in Stewart's wilt.

Literature Cited

Bennion, D., Charleson, E.S., Coon, E., and Misra R. 2010. Dissection of β-barrel outer membrane protein assembly pathways through characterizing BamA PDTRA1 mutants of *Escherichia coli. Molecular Microbiology* 77(5) 153-1171

Beroz, F., Yan, J., Meir, Y., Sabass, B., Stone, H.A., Bassler, B.L., and Wingreen, N.S. 2018. Verticalization of bacterial biofilms. *Nature Physics* 14: 954–960

Brossard, K.A., and Campagnaria, A.A. 2011. The *Acinetobacter baumannii* Biofilm-Associated Protein Plays a Role in Adherence to Human Epithelial Cells. *Infection and Immunity* 228 –233

Burbank, L. 2014. Global Regulation of Virulence Determinants During Plant Colonization in the Bacterial Phytopathogen, *Pantoea stewartii* subsp. *stewartii*. Doctoral Dissertation.

Carlier, A., Burbank, L., and von Bodman, S.B. 2009. Identification and characterization of three novel EsaI/EsaR quorum-sensing controlled stewartan exopolysaccharide biosynthetic genes in *Pantoea stewartii* ssp. *stewartii*. *Molecular Microbiology* 74(4): 903-913.

Castro, C. 2021. Characterization of *Xylella fastidiosa* Lipopolysaccharide-induced Plant Defense Priming, Endoglucanase-regulated Exopolysaccharide Production, and Type IV Pili. Doctoral Dissertation.

Chang, J.H, Desveux, D., and Creason, A.L. 2014. The ABCs and 123s of Bacterial Secretion Systems in Plant Pathogenesis. *Annual Review of Phytopathology* 52:317–45

Chenal, A, Karst, J.C., Perex, A.C.S. Wozniak, A.K., Baron, B., England, P. and Landant, D. 2010. Calcium-Induced Folding and Stabilization of the Intrinsically Disordered RTX Domain of the CyaA Toxin. *Biophysical Journal* 99: 3744-3753.

Cheng, H.-P., and Walker, G.C., 1998. Succinoglycan is required for initiation and elongation of infection threads during nodulation of alfalfa by *Rhizobium meliloti*. *Journal of Bacteriology* 180, 5183–5191.

Ciccarelli, F.D., Copley, R.R., Doerks, T., Russell, R.B. and Bork, P. 2002. CASH – a β-helix domain widespread among carbohydrate-binding proteins. *TRENDS in Biochemical Sciences* 27(2): 59 – 62.

Coplin, D. L., Frederick, R. D., Majerczak, D. R., and Haas, E. S. 1986. Molecular cloning of virulence genes from *Erwinia stewartii*. *Journal of Bacteriology* 168:619-623

Davies, D.G. and Marques, C.N.H. 2009. A Fatty Acid Messenger Is Responsible for Inducing Dispersion in Microbial Biofilms. *Journal of Bacteriology*. 191(5) 1393-1403.

Dossa, S.G., Karlovsky, P. and Wydra, K. 2014. Biochemical Approach for Virulence Factors' Identification in *Xanthomonas oryzae* Pv. *oryzae*. *Journal of Plant Pathology and Microbiology* 5: 222. doi:10.4172/2157-7471.1000222

Fiser, R., and Konopasek, I. 2009. Different modes of membrane permeabilization by two RTX toxins: Hyla from *Escherichia coli* and CyaA from *Bordatella pertussis*. *Biochimica et Biophysica Acta* 1788: 1249-1254

Gambetta, G.A., Matthews, M.A. and Syvanen, M. 2018. The *Xylella fastidiousa* RTX operons: evidence for the evolution of protein mosaics through novel genetic exchanges. *BMC Genomics* 19:329 https://doi.org/10.1186/s12864-018-4731-9

Gumerov, V.M., and Zhulin, I.B. 2020. TREND: a platform for exploring protein function in prokaryotes based on phylogenetic, domain architecture and gene neighborhood analyses, *Nucleic Acids Research*, gkaa243, https://doi.org/10.1093/nar/gkaa243

Ham, J.H., Majerczak, D.R., Arroyo-Rodriguez, A.S., Mackey, D.M., and Coplin D. 2006. WtsE, and AvrE-family effector protein from *Pantoea stewartii* subsp. *stewartii*, causes disease-associated cell death in corn and requites a chaperone protein for stability. *Molecular Plant Microbe Interactions* 19: 1092-1102.

Hartmann R, Jeckel H, Jelli E, Singh PK, Vaidya S, Bayer M, et al. 2021. Quantitative image analysis of microbial communities with BiofilmQ. *Nat Microbiol*. doi:10.1038/s41564-020-00817-4

Hébrard, M., Kröger, C., Srikumar, S., Colgan, A., Händler, K., & Hinton, J.C.D. 2012. sRNAs and the virulence of *Salmonella enterica* serovar Typhimurium. *RNA Biology* 9(4), 437-445, DOI: 10.4161/rna.20480

Heidelberg, J. F., R. Seshadri, S. A. Haveman, C. L. Hemme, I. T. Paulsen, J. F. Kolonay, J. A. Eisen, N. Ward, B. Methe, L. M. Brinkac, S. C. Daugherty, R. T. Deboy, R. J. Dodson, A. S. Durkin, R. Madupu, W. C. Nelson, S. A. Sullivan, D. Fouts, D. H. Haft, J. Selengut, J. D. Peterson, T. M. Davidsen, N. Zafar, L. W. Zhou, D. Radune, G. Dimitrov, M. Hance, K. Tran, H. Khouri, J. Gill, T. R. Utterback, T. V. Feldblyum, J. D. Wall, G. Voordouw, and C. M. Fraser. 2004. The genome sequence of the anaerobic, sulfate-reducing bacterium *Desulfovibrio vulgaris* Hildenborough. *Nature Biotechnol* 22:554-559.

Heipieper, H.J., Pepi, M., Baumgarten, T., and Eberlein, C. 2010. Surface Properties and Cellular Energetics of Bacteria in Response to the Presence of Hydrocarbons. Cellular Ecophysiology of Microbe: Hydrocarbon and Lipid Interactions. Krell, T. (ed.) Spriner 2010. 397-408.

Hinchliffe S.J., Howard S.L., Huang Y.H., Clarke D.J., Wren B.W. 2008. The importance of the Rcs phosphorelay in the survival and pathogenesis of the enteropathogenic *Yersiniae*. *Microbiology* 154:1117–1131

Koutsoudis, M.D., Tsaltas, D., Minogue, T.D., and Von Bodman, S.B. 2006. Quorum-sensing regulation governs bacterial adhesion, biofilm development, and host colonization in *Pantoea stewartii* subspecies *stewartii*. *Proceedings of the National Academy of Sciences* 103: 15 5983-5988

Kovach, M. E., Elzer, P. H., Hill, D. S., Robertson, G. T., Farris, M. A., Roop, R. M., 2nd, and Peterson, K. M. 1995. Four new derivatives of the broad-host-range cloning vector pBBR1MCS, carrying different antibiotic-resistance cassettes. *Gene* 166:175-176

Lahesaare A, Ainelo H, Teppo A, Kivisaar M, Heipieper HJ, Teras R. 2016. LapF and Its Regulation by Fis Affect the Cell Surface Hydrophobicity of *Pseudomonas putida*. *PLoS ONE* 11(11): e0166078. doi:10.1371/journal. pone.0166078

Lasa, I., and Penadés, J.R. 2006. Mini-Review: Bap: A family of surface proteins involved in biofilm formation. *Research in Microbiology* 157: 99–107

Niu, C., and Gilbert, E.S. 2004. Colorimetric Method for Identifying Plant Essential Oil Components That Affect Biofilm Formation and Structure. *Applied and Environmental Microbiology* 70(12): 6951-6956.

O'toole, G.A. 2003. To Build a Biofilm. *Journal of Bacteriology* 185(9): 2687–2689

Roper, M.C., Burbank, L.P., Williams, K., Viravathana, P., Tien, H. and Von Bodman, S. 2015. A large repetitive RTX-like protein mediates water-soaked lesion development, leakage of plant cell content and host colonization in the *Pantoea stewartii* subsp. *stewartii* pathosystem. *Molecular Plant-Microbe Interactions* 12: 1374-1882.

Rosenburg, M. 1984. Bacterial adherence to hydrocarbons: a useful technique for studying cell surface hydrophobicity. *FEMS Microbiology Letter* 22(3): 289-295.

Salanoubat, M., Genin, S., Artiguenave, F., Gouzy, J., Mangenot, S., Arlat, M., Billaultk, A., Brottier, P., Camus, J.C., Cattolico, L., Chandler, M., Choisne, N., Claudel-RenardI, C., Cunnac, S., Demange, N., Gaspin, C., Lavie, Moisan A., Robert, C., Saurin, W., Schiex, T., Siguier, P., Thebault, P., Whalen, M., Wincker, P., Levy, M., Weissenbach, J. Boucher, C.A. 2002. Genome sequence of the plant pathogen *Ralstonia solanacearum*. *Nature* 415: 497- 502.

Satchell, K.J.F. 2011. Structure and Function of MARTX Toxins and other large repetitive RTX proteins. *Annual Review of Microbiology* 65: 71-90

Simon, R., Priefer, U., and Puhler, A. 1983. A Broad Host Range Mobilization Syfflm For In Vivo Genric Engineering: Transposon Mutagenesis in Gram Negative Bacteria. *Biotechnology* 1: 784-791.

Sorroche, F.G., Spesia, M.B., Zorreguieta, A., and Giordano, W. 2012. A Positive Correlation between Bacterial Autoaggregation and Biofilm Formation in Native *Sinorhizobium meliloti* Isolates from Argentina. *Applied and Environmental Microbiology* 78(12). 4092-4101.

Swiatlo, E, Champlin, F.R., Holman, S.C., Wilson, W.W., and Watt, J.M. 2002. Contribution of Choline-Binding Proteins to Cell Surface Properties of *Streptococcus pneumoniae*. *Infection and Immunity* 70(1): 412-415

Tao, K., Z. Long, K. Liu, Y. Tao, and S. Liu. 2006. Purification and properties of a novel insecticidal protein from the locust pathogen *Serratia marcescens* HR-3. *Curr Microbiol* 52:45-9.

Theunissen, S., De Smet, L., Dansercoer, A., Motte, B., Coenye, T., Van Beeumen, J.J., Devreese, B., Savvides, S.N., Vergauwen, B. 2010. The 285 kDa Bap/RTX hybrid cell surface protein (SO4317) of *Shewanella oneidensis* MR-1 is a key mediator of biofilm formation. *Research in Microbiology* 161: 144-152.

Toledo-Arana A, Valle J, Solano C, Arrizubieta, M.J., Cucarella, C. Lamata, M., Amorena, B., Leiva, J., Penade, J.R., and Lasa, I. 2001. The enterococcal surface protein, Esp, is involved in *Enterococcus faecalis* biofilm formation. *Applied Environmental Microbiology* 67:4538–45

Tribedi, P, and Sil, A.K. 2014. Cell surface hydrophobicity: a key component in the degradation of polyethylene succinate by *Pseudomonas* sp. AKS2. Journal of Applied Microbiology 116: 295-303

Zhang, X.S., Garcia-Contrerras, R. and Wood, T.K. 2007. YcfR (BhsA) Influences *Escherichia coli* Biofilm Formation through Stress Response and Surface Hydrophobicity. *Journal of Bacteriology* 189(8): 3051-3062

Chapter III

OxyR Regulates the Rcs Phosphorelay Under Oxidative Stress in the Bacterial Plant Pathogen, *Pantoea stewartii* subsp. *stewartii*

Abstract

Pantoea stewartii subsp. *stewartii*, is the causative agent of Stewart's wilt in sweet corn. This disease is characterized by seedling wilt and water soaked (WS) lesion formation. WS lesions contain high levels of the reactive oxygen species (ROS) likely as a consequence of cellular lysis caused by the bacterium. The transcription factor OxyR plays a significant role in regulating the response to H_2O_2 exposure by sensing and responding to oxidative stress and inducing production of ROS degradative enzymes, like an alkyl hydroperoxidase. Interestingly, in *P. stewartii*, the operator region of an operon that contains components of the Regulator of Capsular Synthesis (Rcs) pathway, that regulates EPS production, contains a conserved OxyR binding site. Moreover, an *ΔoxyR* mutant produces significantly less capsular polysaccharide than the wild type parental strain suggesting that the Rcs phosphorelay and downstream EPS production are tied to sensing of environmental ROS. Our data demonstrate that, indeed, sublethal exposure to the ROS generators, H_2O_2 and paraquat, induced expression of the Rcs operon. Furthermore, promoter binding assays confirmed that OxyR binds to the operator region of this operon. Induction of the Rcs phosphorelay by sensing of ROS via OxyR may be one mechanism *P. stewartii* uses to transition from the WS lesion phase to the xylem phase of plant colonization. This operon also encodes two *rtx* toxin genes, one of which encodes a RTX protein involved in WS lesion formation. Exposure to ROS in WS lesions stimulates expression of this operon and serves as a method for *P. stewartii* to sense ROS in their local environment, stimulating the production of a protective EPS matrix and to begin the biofilm process, aiding in xylem colonization.

Introduction

Reactive Oxygen Species (ROS) are highly reactive molecules that cause damage to cellular molecules. ROS species include hydrogen peroxide (H_2O_2), nitric oxide (NO), oxide anion (O_2^-), peroxynitrite ($ONOO^-$), hydrochlorous acid (HOCl), and hydroxyl radical (OH^-). These unstable molecules oxidize proteins and lipids, damage DNA and can lead to cell death. The thiol-based transcription factor, OxyR, regulates the redox state inside the bacterial cell by activating genes for protection against H_2O_2 (Tao et al., 1991; Green and Paget, 2004; Seo et al., 2015; Burbank and Roper, 2014). Deletion of *oxyR* leads to increased sensitivity to reactive oxygen species, including H_2O_2 (Tao et al., 1991, Burbank and Roper; 2014, Wan et al., 2018). OxyR also regulates some virulence factors that impact autoaggregation and surface adhesion in *Escherichia coli* and *Serratia marcescens*, respectively (Hasman, et al., 1999; Shanks et al., 2007).

Biofilm formation, a communal association of of microorganisms adhered to a surface enables bacteria, in part, to withstand environmental stressors, including ROS. Biofilm formation is a complex coordinated effort that generally follows the developmental regimen of surface attachment, microcolony formation that mature in microcolonies encased in an extracellular matrix. OxyR has been implicated in early steps of biofilm initiation through regulation of the surface adhesion protein, Ag43 in *Escherichia coli* (Schembri et al., 2003). In *P. stewartii*, deletion of *oxyR* causes a significant reduction in capsular or exopolysaccharide (EPS) production suggesting it is involved in transitioning to the later stages of biofilm formation that require tight regulation of EPS synthesis (Burbank and Roper, 2014). An OxyR conserved binding site

is upstream of an operon containing 2 genes that are a part of the Rcs synthesis signaling pathway along with two repeat in toxin (RTX) like proteins. Deletion of the smaller RTX gene (designated *rtx1*) yields no change in phenotype, but deletion of the larger toxin gene (designated *rtx2*) decreases virulence, and water-soaked lesion formation (Roper et al., 2015). Therefore, I hypothesize reactive oxygen species may induce expression of these key components of the Rcs signal transduction system as well as these RTX like toxins, via OxyR leading EPS synthesis for biofilm formation in *Pantoea stewartii*.

The Rcs phosphorelay is required for EPS production in *P. stewartii* but the environmental signals that induces expression or activity of this important and complex signal transduction system is largely unknown. The primary purpose of this research is to determine if reactive oxygen species may act as an external environmental signal that may induce the process of biofilm formation in *P. stewartii* via the Rcs phosphorelay by use of the transcription factor OxyR.

Materials and Methods

Bacterial Strains, Growth Conditions, and Strain Construction. All *P. stewartii* strains were grown on nutrient agar (Difco Laboratories, Detroit) at 28°C and *E. coli* strains were grown on Luria-Bertani (LB) at 37°C. LB broth (Difco Laboratories) was supplemented with 0.2% glucose (final concentration) where indicated. All pertinent strains of *P. stewartii* and *E. coli* are listed in Table 1. When needed and appropriate, the following antibiotics were added to the media: nalidixic acid, 30 µg/ml; or ampicillin,

100 µg/ml (final concentrations). The *E. coli* S17-1λ strain served as a donor for conjugal transfer.

Recombinant OxyR Synthesis: The *oxyR* gene was cloned into the pET101/d-TOPO expression plasmid (Invitrogen; Waltham, MA), then transformed into BL21(DE3)pLysS for synthesis of a recombinant OxyR protein with a C-terminal His-tag under a T7 inducible promoter (Roper, unpublished data). Recombinant OxyR expressing bacteria were initially grown overnight in LB with 100 µg/ml ampicillin (final concentration) at 37°C while shaking at 180 rpm. Cultures were then subcultured 1/100 into fresh media and grown under the same conditions until an absorbance of $OD600_{nm} = 0.5$ was reached. After addition of 1mM IPTG (final concentration), cultures were grown overnight at 28°C (Roper, unpublished data). Bacterial cells were harvested by centrifugation at 5,000 rpm, at 4°C for 10 minutes, and stored at -80°C. Bacterial crude extracts were prepared by resuspending cell pellets to a concentration of 0.2 gram per ml in cell lysis buffer (100 mM Tris HCl, 1 mM EDTA, and NaCl, pH 8.0) containing Halt™ EDTA-free, proteinase inhibitor Cocktail (Reference # 78425, Mfg. Thermo Scientific). Cell slurries then underwent lysozyme treatment at 4°C followed by sonication on ice with a Fisher Scientific 550 Sonic Dismembrator.

A recombinant mutant version of OxyR with a point mutation in the DNA binding domain (formed by changing serine 33 to asparagine (S33N)) was cloned and expressed as described above as a control. This mutation inactivates the helix-turn-helix DNA binding domain of OxyR (Kullik et al., 1995). This mutation was introduced with a

Thermo Scientific Phusion Site Directed Mutagenesis Kit per manufacturer's instructions (Roper, unpublished data).

Promoter Binding Assays: Electrophoretic Mobility Shift Assay (EMSA): To determine if OxyR binds to its predicted binding site upstream of the *rtx1/rtx2/rcsD/rcsB* operon, individual bacterial crude extracts containing either the recombinant, wild type OxyR or the recombinant, mutated OxyR (S33N) were incubated for 30 minutes at room temperature in 30 microliters of binding buffer (10 mM Tris, pH 7.5, 1 mM EDTA, 100mM KCl, 10 mM DTT, 5% vol/vol glycerol, 0.01 mg/ml of Bovine Serum Albumin, final concentration; Hellman and Fried, 2007) containing 1µg poly(dI-dC) and 50 nanograms of a DNA probe. The DNA probe was an approximately 500 bp PCR product containing either the predicted OxyR binding site for the *rtx1/rtx2/rcsD/rcsB* operon or the OxyR binding site upstream of the *aphC* gene found in *P. stewartii*. The DNA probes were synthesized by PCR with a PrimeStar® GXL DNA Polymerase (Mfg. Takara Bio, Cat# R050A), using gene specific primers (Table 3.2) under the following conditions: initial denaturization at 98°C for 1 minute, then denaturization at 98°C for 10 seconds, annealing at either 55°C for the *aphC* gene OxyR binding site control probe or 40°C for the *rtx1/rtx2/rcsD/rcsB* operon predicted OxyR binding site for 15 seconds, then elongation for 1 minute at 68°C for 30 cycles, followed by an extended elongation at 68°C for 5 minutes. The PCR product was purified with a DNA Clean & Concentrator Kit from Zymo Research (Cat# D4003). The entire solution (30 µl) was loaded onto a 5% native acrylamide TAE gel and run for 90 minutes at 76 V. Gels were the stained with

Invitrogen™ SYBR™ Safe DNA Gel Stain (Catalog # S33102) per manufacturer's instructions and read with a Biorad ChemiDoc™ MP Imaging System.

Promoter Binding Assays: DNA-Protein-Interaction (DPI)- Enzyme-Linked Immunosorbent Assay (ELISA): DNA-Protein-Interaction (DPI)-ELISA was performed per Brand et al., 2010, but with following modifications: wells of a Thermo Scientific™ Pierce™ NeutrAvidin Coated Microplate (Catalog #PI151280) were coated with 1.25 pmol of a biotin-labeled, 22 nucleotide, double stranded DNA fragment, containing either the OxyR binding site upstream of the *rtx1/rtx2/rcsD/rcsB* operon, or the *ahpC* gene (encodes alkyl hydroperoxidase), a gene known to be under regulatory control of OxyR by incubating at room temperature for 2 hours. These DNA fragments were oligonucleotides synthesized by IDT (San Diego, California), and biotin labeled with a Thermo Fisher North2South Complete Biotin Random Prime Labeling and Detection Kit (Catalog # 17175) after forming a double stranded DNA fragment in a Biorad T100™ Thermocycler by initially heating the complementary fragments together at 95°C for 5 minutes, then decreasing the temperature by one degree every minute until a temperature of 20°C was reached. Blocking of the wells was performed with 5% milk in Tris Buffered Saline, pH 7.5 with 0.1% Tween 20. A 1:1000 dilution of a mouse, 6X His-Tag, monoclonal antibody conjugated to horseradish peroxidase (Thermofisher Scientific, Catalog # MA1-21315-HRP) was used to detect any bound, OxyR His-tagged protein. Absorbance at 450 nm was measured with an Infinite M Plex Tecan Plate reader.

Gene Expression Reporter Assays: Individual strains wild type DC283 and *ΔoxyR* transformed with either the pFPV25 vector containing the native promoter region of the

rtx1/rtx2/rcsD/rcsB operon (pFPV25::p*rtx2*) upstream of a gene encoding a GFP reporter protein or the pFPV25 empty vector were grown overnight in LB supplemented with 0.2% glucose containing 100 µg/ml ampicillin (final concentration) at 180 rpm at 28°C. Optical density of individual cultures were adjusted to $OD600_{nm}$ = 0.5, then further diluted to 1:10 in fresh medium and aliquoted into individual wells of a sterile, black chimney polystyrene 96-well plate (Catalog number 3603, Mfg. Costar). The plate was incubated at room temperature for 24 hours. Following this, the individual cultures were exposed to either 0.2 µg/ml paraquat, 10 µM H_2O_2 (final concentration) or sterile water (mock controls) and optical density and fluorescence was continued to be monitored for every 15 minutes for 7 hours, a modified process from Pescaretti et al., 2010 with an Infinite M Plex Tecan Plate reader. Experiments were executed for a total of 3 biological replicates, each containing 3 technical replicates. Readings were reported as the ratio of fluorescence to optical density, and analysis was performed per De Jong and Geiselmann (2015). Calculations to determine fluorescence were done as follows: background fluorescence and optical density was subtracted from each treatment or control well. Following this, the ratio of fluorescence/OD 595 nm was calculated for each well. Then the total amount of fluorescence of each well was calculated. Any calculated negative result was given a value equal to zero. Fluorescence was calculated to determine the difference between wells of bacteria exposed to the sublethal ROS species and the wells of bacteria not exposed to the ROS species.

Quantification of Gene Expression Following Sub-Lethal ROS Treatment. Exposure to ROS was performed as previously described (Burbank and Roper, 2014) with the

following modifications: cells were grown in LB supplemented with 0.2% glucose (final concentration). For the ROS challenge, cells were incubated with 0.2 µg/ml paraquat (final concentration) for 15 minutes, or 10 µM H_2O_2 (final concentration) for 5 minutes. Isolation of RNA was performed as described in Burbank and Roper, 2014. Following DNAse treatment, RNA was quantified using Qubit Analysis. Differentiation of gene expression was determined by a custom probe set designed for the Nanostring Gene Expression System (Seattle, WA). Three reference genes, *ffh* (GenBank accession number EHT99250), *proC* (GenBank accession number EHU02233) and *gyrB* (GenBank accession number WP006121375) were used for normalization of gene expression (Burbank and Roper, 2014; Takle et al. 2007; Yu et al., 2016). All RNAs and Nanostring probes were sent to Canopy Biosciences (Hayward, CA) for testing. Analysis of gene expression data was performed by Nanostring nsolver 4.0 data analysis program and expressed as change in fold gene expression compared with *untreated* (Mock) controls.

Results

OxyR Binds the Operator Region of the *rtx1/rtx2/rcsD/rcsB* Operon. We have demonstrated through EMSA and DPI-ELISA that bacterial crude extracts containing a recombinant version of OxyR binds to a predicted binding operator region of the *rtx1/rtx2/rcsD/rcsB* operon (Figure 3.1 and 3.2). This same bacterial crude extract is also bound to an OxyR transcriptional binding site for the gene *ahpC* that is known to be under control of OxyR that was used as a positive control (Burbank and Roper, 2014). In addition, crude extracts containing a mutated version of the His-tagged recombinant

OxyR that prevents the OxyR protein from binding to DNA did not effectively bind to the operator region of the *rtx1/rtx2/rcsD/rcsB* operon or the operator region of the *ahpC* gene as compared to the wild type recombinant OxyR.

OxyR Induces Expression of the *rtx1/rtx2/rcsD/rcsB* Operon. Wild type and *ΔoxyR* mutant strains of *P. stewartii* containing the plasmid pFPV25::p*rtx2* that included the predicted binding site of OxyR upstream of a GFP reporter were monitored for fluorescence in proportion to optical density, after the introduction of sublethal concentrations of either H_2O_2 or paraquat. These measurements were also compared to untreated strains, as well as empty vector controls. After the introduction of (final concentration) either 10 µM H_2O_2 (Figure 3.3A) or 0.2 µg/ml Paraquat (Figure 3.3B), wild type *P. stewartii* showed a significant increase in fluorescence in proportion to optical density, when compared to the *ΔoxyR* mutant. This was not observed in the *ΔoxyR* strain containing the empty pFPV25::p*rtx2* reporter plasmid, after treatment with H_2O_2 or paraquat. This data also indicates that OxyR does bind to the operator region of the *rtx1/rtx2/rcsD/rcsB* operon.

We also monitored OxyR-dependent induction of gene expression of genes that are controlled by the Rcs phosphorelay following exposure to sub-lethal amounts of H_2O_2 using Nanostring probes designed for genes in the *rtx1/rtx2/rcsD/rcsB* operon, as well as certain possible transcriptional variants that can be detected with the Nanostring technology and methodology. Genes involved in EPS synthesis and flagellar activity were also targeted (Figure 3.4; Tables 3.3 and 3.4).

After sublethal exposure to H_2O_2, Wild type *P. stewartii* showed increased in induction of expression of *ahpC* that is not seen in the *oxyR* mutant (Figure 3.4A). This gene served as a control in the EMSA and DPI-ELISA experiments, as well as in previous publications from the Roper Lab (Burbank, and Roper, 2014). Wild type *P. stewartii* also had an increase in induction of expression of *wceG1,* which encodes a undecaprenyl-phosphate UDP-galactose phosphotransferase required for capsule synthesis (Burbank and Roper, 2014; Kaszowska et al., 2021). This gene is a part of the *wce-I* gene cluster, one of three gene clusters used by *P. stewartii* for EPS synthesis (Carlier et al., 2009). The *ΔoxyR* mutant showed significant decreases in expression of *flhD* and *flhC* genes following hydrogen peroxide exposure as compared to the wild type. Both of these genes encode proteins that form a protein complex that forms a transcriptional activator of the flagellar regulon (Liu and Matsumura, 1994). Both strains of *P. stewartii* showed an increase in expression of *soxS* after non-lethal exposure to hydrogen peroxide. SoxS is important for protection against oxidative stress (Wang et al, 2020; Figure 3.4A).

Sub-lethal exposure to the ROS generator paraquat caused induction of the *rtx1*, *rtx2*, and *rcsD* genes, as well as *wzx2* and *wceo* in wild type *P. stewartii* (Figure 3.4B). The gene *wzx2* encodes a flippase, required for the translocation of lipid-linked repeating units across the inner membrane into the bacterial periplasm, while the *wceo* gene encodes a beta-1,6-glucosyltransferase, required for EPS synthesis (Carlier et al., 2009). Also both *wceG2* and *wceG1* showed increased induction of expression. Both of these genes encode a undecaprenyl-phosphate UDP-galactose phosphotransferase required for

capsule synthesis (Burbank and Roper, 2014; Kaszowska et al., 2021). The *rtx1* gene encodes a hypothetical protein, while *rcsD* encodes for a phoshotransferase and *rcsB* a cytoplasmic response regulator. Both products of the *rcsD* and *rcsB* genes are components of the Rcs phosphorelay (Burbank, 2014). The gene *rtx*2 encodes for a unique RTX-like protein (Roper et al., 2015; Viravathana Chapter 1)

Table 3.1. Bacterial Strains and Plasmids

Strain or Plasmid	Relevant Genotypes	Source
Pantoea stewartii subsp. *stewartii*		
DC283	Wild type, NaI^r	Coplin et al. 1986
Δ*rtx2* (CR54)	NaI^r, gene deletion of *rtx2*	Roper et al., 2015
Δ*oxyR* (LB003)	NaI^r, deletion of *oxyR*	Burbank and Roper, 2014
Escherichia coli		
BL21(DE3)pLysS		Life Sciences, Inc.
S17ʎ	RP4, Mob+, Smr	Simon et al. 1983
Plasmids		
pFPV25	amp^r	Valdivia and Falkow,1996
pFPV25::p*rtx*	amp^r	This Study
pET101	amp^r	Invitrogen

Table 3.2. Primers and Probes used in this study

Primer	Sequence	Source or Reference
oxyR D-topo fwd	CACCATGTTCAGATTCGTTACGCT	This Study
oxyR D-topo rev	AACCGCCTGTTTTAGCGTGG	This Study
ahpC promoter fwd	GTCCAGCTCAGCCACTAAA	This Study
ahpC promoter rev	GACATGTGATGGCCTCCTT	This Study
rtx1_prom-FP500	CGTAGATGGATTTTCGC	This Study
rtx1_prom-RP500	GCGAATCTAAAAACG	This Study
Probe	**Sequence**	**Source or Reference**
rtx1-R-Probe-22	AATTTCGGATTAATTAAAATTA	This Study
rtx1-R-Probe-C22	TAATTTTAATTAATCCGAAATT	This Study
ahpC-R-Probe-22	GGCCTCCTTTAAAATATGTGAT	This Study
ahpC-R-Probe-C22	ATCACATATTTTAAAGGAGGCC	This Study

Table 3.3. Nanostring® Probes used in this study

Gene Name	Gene Product	Accesion Number	ASAP ID
rtx1	hypothetical protein	EHT99805.1	ACV-0291982
rtx2	large Repetitive Protein	EHT99806.1	ACV-0285925
wceG2(*WbaP*)	undecaprenyl-phosphate UDP-galactose phosphotransferase	WP_006119430.1	ACV-0286879
wzx2	flippase	WP_006118652.1	ACV-0288192
wceo	beta-1,6-glucosyltransferase	WP_006118651.1	ACV-0288191
wceG1(*WbaP*)	undecaprenyl-phosphate UDP-galactose phosphotransferase	WP_006119874.1	ACV-0289544
rcsD	phosphotransferase	WP_006120000.1	ACV-0285924
rcsB	DNA-binding response regulator in two-component regulatory system with RcsC & YojN	Not Available	ACV-0285923
wzc	tyrosine-protein kinase	WP_006119870.1	ACV-0289539
wceB	exopolysaccharide biosynthetic glycosyltransferase	Not Available	ACV-0289537
wzb	phosphotyrosine-protein phosphatase	Not Available	ACV-0289540
soxS	AraC family transcriptional regulator	EHT98349.1	ACV-0288908
wza	polysaccharide export protein	Not Available	ACV-0289541
IrhA	transcriptional regulator LrhA	Not Available	ACV-0285895
flhD	DNA-binding transcriptional dual regulator with FlhC	WP_006119910.1	ACV-0285679
ahpF	FAD/NAD(P)-binding alkyl hydroperoxide reductase, F52a subunit	Not Available	ACV-0289585
ahpC	alkyl hydroperoxide reductase, C22 subunit	EHU00213.1	ACV-0289586
flhC	DNA-binding transcriptional dual regulator with FlhD	Not Available	ACV-0285678
gyR	DNA gyrase, subunit B	WP_006121375.1	ACV-0286312
ffh	Signal Recognition Particle (SRP) component with 4.5S RNA (ffs)	EHT99250.1	ACV-0291041
proC	NAD(P)-binding pyrroline-5-carboxylate reductase	EHU02233.1	ACV-0287596

Table 3.4. Nanostring® Probes used in this study that target possible transcriptional variants of *rtx1/rtx2/rcsD/rcsB* operon

Gene Name	Gene Product	Accesion Number	ASAP ID
rtx2/rcsD	Not Available	Not Available	Not Available
rcsD/rcsB	Not Available	Not Available	Not Available
rtx1/rtx2	Not Available	Not Available	Not Available

A

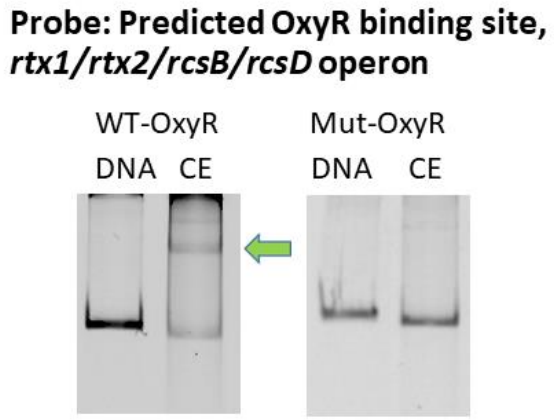

B

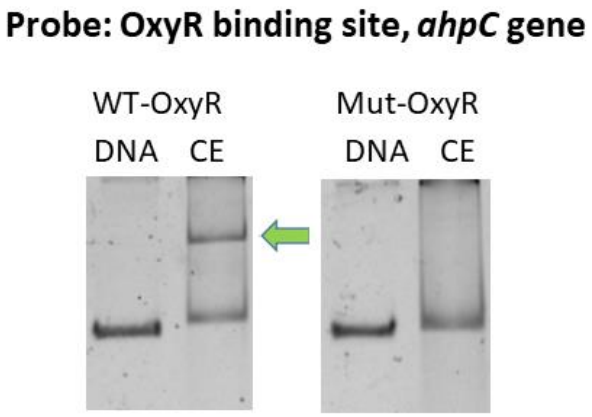

Figure 3.1. OxyR binds to a double stranded DNA probe containing a predicted OxyR binding site upstream of *rtx1/rtx2/rcsD/rcsB* operon. Interaction of OxyR to a predicted OxyR binding site upstream of *rtx1/rtx2/rcsD/rcsB* operon is confirmed via Electrophoretic mobility shift assay (EMSA). A) Bacterial crude extracts (CE) containing recombinant OxyR (WT-OxyR) decreased the distance traveled of dsDNA probe containing a predicted OxyR binding site upstream of the *rtx1/rtx2/rcsD/rcsB* operon as well as (B) the probe containing the OxyR binding site for the *ahpC* downstream control. See green arrows. Crude extracts containing recombinant OxyR with a mutated DNA binding site (Mut-OxyR) negated the decrease in the distance that both probes travelled.

A

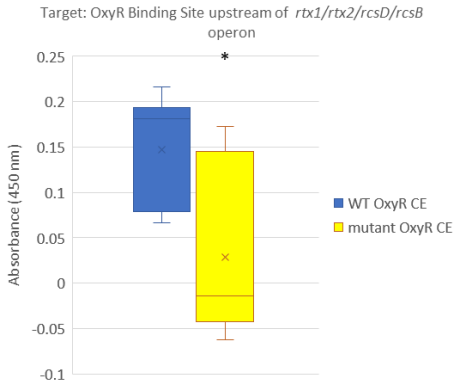

B

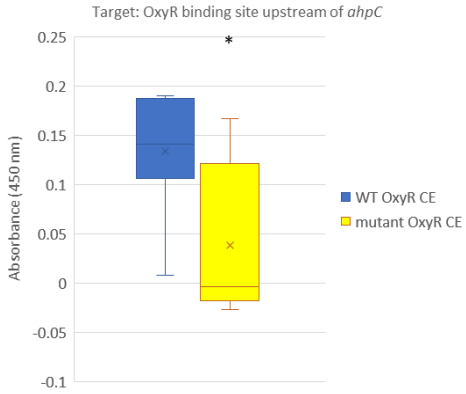

Figure 3.2 DNA-Protein-Interaction (DPI)-ELISA detects significant presence of His-tagged recombinant OxyR in bacterial crude extracts. Bacterial crude extracts containing wild type, recombinant OxyR (WT OxyR CE) in wells coated with a 22 nucleotide, double stranded, biotinylated DNA containing either the predicted predicted OxyR binding site upstream of *rtx1/rtx2/rcsD/rcsB* operon (A) or the OxyR binding site upstream of the gene *ahpC* (downstream control; B) were detected by His-tagged Antibody. There is a significant decrease in presence of His-tagged recombinant OxyR when a mutation is introduced in the DNA binding site (mutant OxyR CE). Results are based on 3 biological replicates, each with 3 technical replicates with 100 micrograms of bacterial crude extract being loaded into each well. Background absorbance (no bacterial crude extracts) was deducted from all readings before calculation. There was no significant difference between background absorbance and readings of bacterial crude extracts in wells that were not not coated with biotinylated, double stranded DNA (data not shown). Asterick denotes significance of $p < 0.05$ via t-test.

A

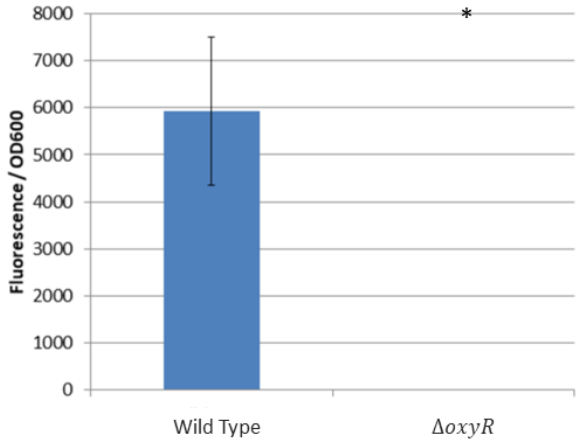

B

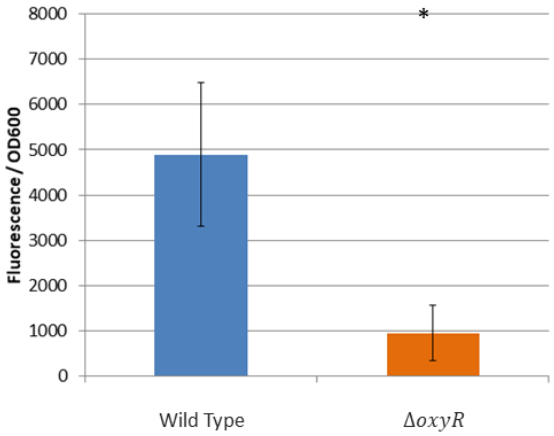

Figure 3.3. Reporter assays indicate that sublethal exposure of reaction oxygen species induces promotor activity via the transcription factor OxyR. Exposure to A) 10 µM of hydrogen peroxide or B) 0.2 µg/ml of the ROS generator paraquat demonstrates an increase in fluorescence in proportion to bacterial optical density in wild type *P. stewartii* containing the plasmid pFPV25::p*rtx*. A significant increase in fluorescence in proportion to optical density was not seen in the *P. stewartii ΔoxyR* containing the pFPV25::*rtx* plasmid. * indicates significance of p = 0.03 while ** indicates p = 0.001 via t-test Results are based on 3 biological replicates, each with 3 technical replicates.

A

	Strain	
Gene Name	Wild Type	*ΔoxyR*
rtx2/rcsD	-0.803	-1.07
rcsD/rcsB	0.0571	-0.227
rtx1	-0.689	0.338
rtx2	-0.486	0.883
wceG2 (WbaP)	-0.951	-0.561
rtx1/rtx2	-0.54	0.28
wzx2	-0.916	-0.129
wceo	-0.953	-0.345
wceG1(WbaP)	1.64	-1.07
rcsD	-0.366	-0.3
rcsB	0.125	-0.132
wzc	-0.418	-0.185
wceB	0.0686	0.0568
wzb	-0.302	0.367
soxS	2.98	2.63
wza	-0.448	-0.187
lrhA	0.452	-0.0896
flhD	-0.923	-1.19
ahpF	2.72	-0.0624
ahpC	2.49	0.417
flhC	-0.819	-0.89

B

	Strain	
Gene Name	Wild Type	*ΔoxyR*
rtx2/rcsD	0.699	0.509
rcsD/rcsB	0.573	0.76
rtx1	1.25	0.699
rtx2	1.1	0.811
wceG2 (WbaP)	1.11	0.844
rtx1/rtx2	1.06	0.5
wzx2	0.849	0.577
wceo	0.942	0.995
wceG1 (WbaP)	1.22	0.837
rcsD	0.325	0.157
rcsB	0.195	0.236
wzc	1.01	0.615
wceB	0.759	0.588
wzb	0.891	0.651
soxS	-0.917	0.308
wza	0.904	0.614
lrhA	-0.228	-0.127
flhD	0.307	-0.0143
ahpF	0.18	0.123
ahpC	0.123	0.0989
flhC	0.13	-0.199

Figure 3.4. Fold change gene expression in the *rtx1/rtx2/rcsD/rcsB* operon and biofilm related genes via OxyR after sublethal exposure to reactive oxygen species. A) Fold change in level of gene expression after sub-lethal exposure to 10 µM H_2O_2 and B) Fold change in gene expression after sublethal exposure to 0.2 µg/ml of paraquat. Numbers denote log2 fold change comparing treated vs non-treated (Mock) bacteria cells, red color denotes no significant change in gene expression, while green color indicates significant fold change indicated by $p < 0.05$ via t-test by analysis with Nanostring nsolver 4.0 data analysis program.

Discussion

Bacterial protection against reactive oxygen species is vital for its survival. The highly unstable compounds that are Reactive Oxygen Species (ROS) are a significant danger to cellular molecules. These compounds, such as hydrogen peroxide (H_2O_2), and superoxides (O_2^-) oxidize proteins, lipids, proteins, and DNA. The damage caused can lead to cell death. Bacterial species have evolved a variety of methodologies to protect themselves from this danger.

The transcription factor, OxyR, induces expression of genes required for protection against H_2O_2 and to maintain the proper redox state inside the bacterial cell (Tao et al., 1991; Green and Paget, 2004; Seo et al., 2015; Burbank and Roper, 2014). In the human pathogen *Klebsiella pneumoniae*, OxyR is vital in combating oxidative stress and in pathogenesis by enhancing fimbrial expression, mucosal colonization, and biofilm formation, allowing for gastrointestinal colonization. The deletion of *oxyR* resulted in higher sensitivity to bile and acid stresses (Hennequin and Forestier, 2009). However, in the soil dwelling gram negative bacterium *Acinetobacter oleivorans* DR1, and the obligate anaerobe, periodontal pathogen *Tannerella forsythia*, the deletion of *oxyR* increases EPS production (Jang et al., 2016; Shin et al., 2020, Honma et al., 2009) . The deletion of *oxyR* also decreases cell-cell aggregation in *T. forsythia* (Honma et al., 2009). A similar observation is seen in *Escherichia coli* where deletion of *oxyR* decreases the expression of the Antiaggregation Factor 43, leading to a decrease in clumping and fluffing of cells needed for biofilm formation (Schrembi et al, 2003).

In *Pantoea stewartii*, the transcription factor OxyR not only confers resistance to oxidative stress, but is required for full EPS production (Burbank and Roper, 2014). Here, we have shown that OxyR also induces expression of the gene *rcsD*, which encodes a phosphotransferase that is a part of the Rcs phosphorelay, a high conserved signal transduction system that regulates EPS production. OxyR also induces expression of other components of that operon, particularly the gene *rtx2*. The *rtx2* gene encodes a unique RTX-like protein required for the formation of water-soaked lesion formation and is vital for biofilm formation (Roper et al., 2015, Viravathana, Chapter 1 and 2).

One of the most important functions of the Rcs phosphorelay is to regulate the synthesis of exopolysaccharide (Majdalani and Gottesman, 2005). The terminal receiver of phosphate groups in this system: the cytoplasmic response regulator RcsB forms a heterodimer with the auxillary response regulator RcsA to induce expression of genes vital for EPS synthesis (Pristovsek et al., 2003).

Exopolysaccharide synthesis is a highly regulated and resource intensive process. Even subtle differences in the environment can lead to unwanted changes in these processes. *In-vitro*, wild type *P. stewartii* produces excess EPS, which may prevent and mask cell to cell and adhesion interactions (Koutsoudis, et al., 2006). Further regulation of the Rcs phosphorelay is thru the repression of *rcsA* by the EsaI/EsaR quorum sensing system. Only after a significant cell density is established, then will concentrations of EsaI be high enough to hinder EsaR repression of the induction of expression of *rcsA* (Von Bodman et al. 1998; Minogue et al., 2005). This coordinated regulation between the

Rcs phoshorelay and the EsaI/EsaR quorum sensing system allows for EPS synthesis to proceed only at the most proper time in biofilm formation.

Here I have shown that *in-vitro*, induction of gene expression of portion(s) of the *rtx1/rtx2/rcsD/rcsB* operon are dependent on transcription factor OxyR, after the sub-lethal exposure of Reactive Oxygen Species. Overall, published information on what induces expression of genes of the components of the Rcs phoshphorelay remains limited. In *Salmonella*, increased expression of *rcsB*, negatively impacts expression of *rcsD*. Also, while *rcsD* and *rcsB* are located in their own operon, the differental expression of *rcsD* and *rcsB* is due to the regulation of two different promoters of two promoters for *rcsB* (Pescaretti et al., 2010).

Genome organization of major components of the Rcs phosphorelay is mostly conserved among members of the family Enterobacteriaceae. In order, genes *rcsD* and *rcsB* are adjacent, with *rcsC* downstream in the opposite orientation (Dehal, et al. 2009). There is a nonconical and unique arrangement to certain genes of the Rcs phosphorelay in *Pantoea stewartii*: the *rcsD* and *rcsB* genes are found in an operon with two genes that encode rtx-like toxins.

This distinct arrangement of the Rcs phosphorelay, as well as the presence of the the two genes that encode rtx-like toxins in the same operon can provide the unique opportunity to study the functions of the Rcs phosphorelay that can be applied to other members of the Family Enterobacteraicee. Additional experiments to determine the true correlation between OxyR, RTX2 and exopolysaccharide production, as well as the identification of transcript variants of the *rtx1/rtx2/rcsD/rcsB* operon are vital to decipher

the relationship between these two vital proteins in the infection process of *P. stewartii* to corn seedlings.

Literature Cited

Brand, L.H., Kirchler, T., Hummel, S., Chaban, C., and Wanke, D. 2010. DPI-ELISA: a fast and versatile method to specify the binding of plant transcription factors to DNA in vitro. *Plant Methods* 6:25.

Burbank, L. and Roper, M.C. 2014. OxyR and SoxR Modulate the Inducible Oxidative Stress Response and Are Implicated During Different Stages of Infection for the Bacterial Phytopathogen *Pantoea stewartii* subsp. *stewartii*. *Molecular Plant-Microbe Interactions* 27(5): 479-490.

Burbank, L. 2014. Global Regulation of Virulence Determinants During Plant Colonization in the Bacterial Phytopathogen, *Pantoea stewartii* subsp. *stewartii*. Doctoral Dissertation.

Carlier, A., Burbank, L., and von Bodman, S.B. 2009. Identification and characterization of three novel EsaI/EsaR quorum-sensing controlled stewartan exopolysaccharide biosynthetic genes in *Pantoea stewartii* ssp. *stewartii*. *Molecular Microbiology* 74(4), 903–913

Coplin, D. L., Frederick, R. D., Majerczak, D. R., and Haas, E. S. 1986. Molecular cloning of virulence genes from *Erwinia stewartii*. *Journal of Bacteriology* 168:619-623

De Jong, H., and Geiselmann, J. 2015. Fluorescent Reporter Genes and the Analysis of Bacterial Regulatory Networks. HSB 2013 and 2014, LNBI 7699, 27-50.

Dehal, P. S., Joachimiak, M. P., Price, M. N., Bates, J. T., Baumohl, J. K., Chivian, D., Friedland, G. D., Huang, K. H., Keller, K., Novichkov, P.S., Dubchak, I. L., Alm, E. J., and Arkin, A. P. 2009. MicrobesOnline: an integrated portal for comparative and functional genomics. *Nuc. Acids Res*. DOI: 10.1093/nar/gkp919

Green, J., and Paget, M.S. 2004. Bacterial Redox sensors. *Nature* 2: 954-967.

Hasman, H., Chakraborty, T., and Klemm, P. 1999. Antigen-43-Mediated Autoaggregation of *Escherichia coli* Is Blocked by Fimbriation. *Journal of Bacteriology* 181(16): 4834-4841

Hellman, L.M., and Fried, M.G. 2007. Electrophoretic mobility shift assay (EMSA) for detecting protein–nucleic acid interactions. *Nature Protocols* 2(8): 1849-1861.

Hennequin, C and Forestier, C. 2009. *oxyR*, a LysR-Type Regulator Involved in *Klebsiella pneumoniae* Mucosal and Abiotic Colonization**.** *Infection and Immunity* (77) 12 5449-5457 https://doi.org/10.1128/IAI.00837-09

Honma,K., Mishima, E., Inagaki, S. and Sharma, A. 2009. The OxyR homologue in *Tannerella forsythia* regulates expression of oxidative stress responses and biofilm formation. *Microbiology* 155. 1912–1922 DOI 10.1099/mic.0.027920-0

Jang, I, Kim, J., and Park, W. 2016. Endogenous hydrogen peroxide increases biofilm formation by inducing exopolysaccharide production in *Acinetobacter oleivorans* DR1. Sci. Rep. 6, 21121; doi: 10.1038/ srep21121

Kaszowska, M., Majkowska-Skrobek, G., Markwitz, P., Lood, C., Jachymek, W., Maciejewska, A., Lukasiewicz, J., Drulis-Kawa, Z. 2021. The Mutation in wbaP cps Gene Cluster Selected by Phage-Borne Depolymerase Abolishes Capsule Production and Diminishes the Virulence of *Klebsiella pneumoniae*. *Int. J. Mol. Sci*. 22: 11562. https:// doi.org/10.3390/ijms222111562

Koutsoudis, M.D., Tsaltas, D., Minogue, T.D., and Von Bodman, S.B. 2006. Quorum-sensing regulation governs bacterial adhesion, biofilm development, and host colonization in *Pantoea stewartii* subspecies *stewartii*. *Proceedings of the National Academy of Sciences* 103: 15 5983-5988

Kullik, I, Toledano, M.B., Tartaglia, L.A., Storz, A. 1995. Mutational Analysis of the Redox-Sensitive TranscriptionalRegulator OxyR: Regions Important for Oxidationand Transcriptional Activation. *Journal of Bacteriology* 177(5): 1275-1284.

Liu, X., and Matsumura, P. 1994. The FlhD/FlhC Complex, a Transcriptional Activator of the *Escherichia coli* Flagellar Class II Operons. *Journal of Bacteriology* 176(23): 7345-7351.

Majdalani N., and Gottesman S. 2005. The Rcs Phosphorelay: A Complex Signal Transduction System. *Annual Review of Microbiology* 59: 379-405

Minogue, T.D., Carlier, A.L., Koutsoudis, M.D., and Von Bodman, S.B. 2005. The cell density-dependent expression of stewartan exopolysaccharide in *Pantoea stewartii* ssp. *stewartii* is a function of EsaR-mediated repression of the *rcsA* gene. *Molecular Microbiology* 56(1): 189-203

Pescaretti, M.d.M., Lopez, F.F., Morero, R.D., and Delgado, M.A. 2010. Transcriptional autoregulation of the RcsCDB phosphorelay system in *Salmonella enterica* serovar *Typhimurium*. *Microbiology* 156: 3513–3521

Pristovsek P, Sengupta K, Lohr F, Schafer B, Von Trebra M.W., Ruterjans, H. and Bernhard, F. 2003. Structural analysis of the DNA-binding domain of the *Erwinia amylovora* RcsB protein and its interaction with the RcsAB box. *Journal of Biological Chemistry* 278:17752–59

Roper, M.C., Burbank, L.P., Williams, K., Viravathana, P., Tien, H. and Von Bodman, S. 2015. A large repetitive RTX-like protein mediates water-soaked lesion development, leakage of plant cell content and host colonization in the *Pantoea stewartii* subsp. *stewartii* pathosystem. *Molecular Plant-Microbe Interactions* 12: 1374-1882.

Schrembi, M.A., Hjerrild, L., Gjermansen, M. and Klemm, P. 2003. Differential Expression of the *Escherichia coli* Autoaggregation Factor Antigen 43. *Journal of Bacteriology* 185(7): 2236-2242

Seo, S.W., Kin, D., Szubin, R., and Palsson, B.O. 2015. Genome-wide Reconstruction of OxyR and SoxRS Transcriptional Regulatory Networks under Oxidative Stress in *Escherichia coli* K-12 MG1655. *Cell Reports* 12: 1289-1299.

Shanks, R.M.Q, Stella, N.A., Kalivoda, E.J., Doe, M.R., O'Dee, D.M., Lathrop, K.L., Guo, F.L., and Nau, G.J. 2007. A *Serratia marcescens* OxyR Homolog Mediates Surface Attachment and Biofilm Formation. *Journal of Bacteriology* 189(20): 7262-7272.

Shin, B., Park, C., and Park, W. 2020. OxyR-controlled surface polysaccharide production and biofilm formation in Acinetobacter oleivorans DR1. Applied Microbiology and Biotechnology 104:1259–1271 https://doi.org/10.1007/s00253-019-10303-5

Simon, R., Priefer, U., and Puhler, A. 1983. A Broad Host Range Mobilization Syfflm For In Vivo Genric Engineering: Transposon Mutagenesis in Gram Negative Bacteria. *Biotechnology* 1: 784-791.

Takle, G. W., Toth, I. K., and Brurberg, M. B. 2007. Evaluation of reference genes for real-time RT-PCR expression studies in the plant pathogen Pectobacterium atrosepticum. BMC Plant Biology. 7:50

Tao, K., Makino, K., Yonei, S., Nakata, A., and Shinagawa, H. 1991. Purification and Characterization of the *Escherichia coli* OxyR Protein, the Positive Regulator for a Hydrogen Peroxide-Inducible Regulon. *Journal of Biochemistry* 109: 262-266.

Valdivia R.H., Falkow S. 1996. Bacterial genetics by flow cytometry: rapid isolation of *Salmonella typhimurium* acid-inducible promoters by differential fluorescence induction. *Mol Microbiol*. 22(2):367-78.

Von Bodman, S., Majerczak, D.R., and Coplin, D.L. 1998. A negative regulator mediates quorum-sensing control of exopolysaccharide production in *Pantoea stewartii* subsp. *stewartii*. *Proceedings of the National Academy of Sciences* 95: 7687-7692

Wan, F., Kong, L., and Gao, H. 2018. Defining the binding determinants of *Shewanella oneidensis* OxyR: implications for the link between the contracted OxyR regulon and adaptation. *J. Biol. Chem.* 293, 4085–4096. doi: 10.1074/jbc. RA117.001530

Wang, P., Zhang, H, Liu, Y., Lv, R., Liu, X., Song, X., Wang, J., Jiang, L., 2020. SoxS is a positive regulator of key pathogenesis genes and promotes intracellular replication and virulence of *Salmonella Typhimurium*. *Microbial Pathogenesis* 139. 103925.

Yu, C., Wang, N., Wu, M., Tian, ,F., Chen, H., Yang, F., Yuan, X., Yang, C., He, C. 2016. OxyR-regulated catalase CatB promotes the virulence in rice via detoxifying hydrogen peroxide in *Xanthomonas oryzae* pv. *oryzae*. *BMC Microbiology* 16:269 DOI 10.1186/s12866-016-0887-0

Appendix

Supplementary Experiments for Research Chapters

Introduction

This section contains supplementary experiments that were part of Chapters 2 and 3.

Materials and Methods

Note: Portion(s) of this section are the same as in Chapters 2 and 3 of this document.

Polymyxin B Challenges in Supplemented AB Medium. Growth Inhibition. Single colonies of wild type, and Δ*rtx2*, *P. stewartii* were grown overnight in AB medium (Clark and Maaloe, 1967) supplemented with 0.2% glucose and 0.05% yeast extract. The following day, cultures were diluted 1/20 and inoculated into fresh AB medium supplemented with 0.2% glucose and 0.05% yeast extract in 96-well U-bottom microplates (Mfg. Falcon, Ref #353077) to a final volume of 150 µl. Cells were treated with final concentrations of Polymyxin B (0 µg/ml, 6.25 µg/ml, 12.5 µg/ml, and 25 µg/ml). Growth was assessed in a Tecan Infinite F200 microplate reader using an absorbance reading of OD_{595nm}. Measurements were taken every hour for 23 hours at room temperature, with 30 seconds of orbital shaking with an amplitude of 6 mm prior to each reading. Growth curve readings are based on 3 biological replicates, each containing 3 technical replicates. To evaluate overall survival, *Δrtx2* and wild type cells that were challenged with polymyxin B as described above were serially diluted with 1X phosphate buffered saline (PBS, pH7.4), plated onto nutrient agar with nalidixic acid (final concentration: 30 µg/ml), and incubated at 28°C for 2 days. The same concentrations of polymyxin B were used as for the growth curve (0, 25, 12.5, and 6.25 µg/ml). Percent

survival was determined by dividing viable cell counts of antibiotic challenged bacteria by mock (negative control) viable cell counts. Results are based on 3 biological replicates, each containing 3 technical replicates.

Surface Adhesion Assays with Poly-Lysine Coated Plates. Adhesion assays were based on Koutsoudis et al., 2006 and Theunissen et al. 2010. In brief, single colonies of wild type, Δ*rtx2*, Δ*wceo*, and Δ*wceo*/Δ*rtx2* were grown at 30°C in LB broth supplemented with 0.2% glucose at 180 rpm. Overnight cultures were all adjusted to OD_{600} = 0.5, then diluted 1/10 in fresh LB broth supplemented with 0.2% glucose and inoculated into a 96-well, Poly-L-Lysine-coated Microplate (Corning; Ref #354516) to a final volume of 150 µl per well. Cells were incubated statically at 28°C for 2 hours. Planktonic cells and culture medium were removed and remaining surface-attached cells were adhered by incubation at 37°C for 60 minutes. 200 µl of a 1% crystal violet solution (solution dissolved in water and filtered through a 0.2-micron filter) was then added to each well and the plates were incubated at room temperature for an hour. The crystal violet solution was removed and each well was then washed three times with sterile water and dried overnight. The crystal violet was then solubilized by adding 200 µl of a 30% Acetic Acid solution per well, followed by a 1 hour shaking period. Absorbance reading were taken at OD595nm in a Tecan Infinite F200 microplate reader. The Adhesion value or Specific Biofilm formation (SBF): growth normalized biofilm accumulation was calculated as follows: (OD595CV-media value)/(OD595Cell growth-media value; Niu and Gilbert, 2004). Results are based on 5 biological replicates, each containing no less than 5 technical replicates**.**

Quantification of Gene Expression After Sub-lethal ROS Treatment. Exposure to ROS performed as previously described (Burbank and Roper, 2014) with the following modifications: cells were grown in Luria Broth with 0.2% glucose. For challenge against ROS species, cells were incubated with 0.2 µg/ml paraquat (final concentration) for 15 minutes, or 10 µM H_2O_2 (final concentration) for 5 minutes. Differentiation of gene expression was determined by TaqMan quantitative (q) PCR assays. Primers and probes for TaqMan qPCR were designed and optimized using Beacon design software (Mfg. Premier Biosoft). Two reference genes, *ffh* (GenBank accession number EHT99250) and *proC* (GenBank accession number EHU02233) were used for normalization of gene expression (Burbank and Roper, 2014; Takle et al. 2007). Analysis of qPCR data was performed by CFX Manager software (Biorad Laboratories) and expressed as change in fold gene expression compared with untreated (mock) controls. Results are based on 3 biological replicates, each with 3 technical replicates.

Results

Polymyxin Challenge in AB Medium Showed No Difference Versus use of Luria Broth With 0.2% Glucose. Growth curves challenged against varying concentration of the antibiotic Polymxyin B of A) wild type *P. stewartii* and B) Δ*rtx2* mutant as well as End Point Plate Counts demonstrated that the deletion of Δ*rtx2* compromises membrane integrity when compared to the wild type under all concentrations tested (Figure A.1A, A.1B, and A.1C).

Surface Adhesion in Poly-Lysine Coated Plates is Impacted by the Deletion of *rtx2* in a Non-EPS Producing Background. RTX2 is a large (249.8 kDa) protein containing 5 putative Ca^{2+}-binding domains similar to serralysin, from *Serratia marcescens* and a hemolysin-like protein from *Desulfovibrio vulgaris*. It also has 5 predicted transmembrane domains in the C-terminus, and large repetitive adhesin motifs homologous to hemagglutinins and to the BAP subfamily of RTX proteins implicated in promoting bacterial-host adhesion during biofilm formation (Roper et al., 2015). In a wild type (EPS-producing background), there was no significant difference between wild type and the Δ*rtx2* in adhesion in proportion to optical density growth (Absorbance value). However, in a non-EPS producing genetic background (Δ*wceo*), deletion of *rtx2* (Δ*wceo*/Δ*rtx2*) reduces surface adhesion compared to the wild type (Δ*wceo*). The non-EPS producing wild type *(Δwceo*) had a higher adhesion value than all other tested strains (Figure A.2), similar to what is seen with the use of acetone treated, non-coated, polystyrene microplates (Viravathana, Chapter 2)

***In Vitro* Induction of *rcsD* is OxyR-Dependent**. Using TaqMan® based qPCR, there was only a significant increase in the induction of gene expression for r*csD* in wild type *P. stewartii* and not in the Δ*oxyR* mutant when grown in Luria Broth with 0.2% glucose, after sub-lethal expsoure to 10 µM of hydrogen peroxide for 5 minutes (Figure A.3). However, both *rcsB* and *rcsD* demonstrated higher levels of expression in wild type *P. stewartii* versus Δ*oxyR* when exposed to 0.2 µg/ml of paraquat for 15 minutes, when also grown in Luria broth with 0.2% glucose (Figure A.4).

Table A.1 Primers and Probes used in this study

Primer	Sequence	Source or Reference
rcsD RT FP2	CCTTGAGACAACCCAGGTTTCG	This study
rcsD RT RP2	CGAGCAGCAGGCGAACAAG	This study
rcsB RT FP	GAAGGTATCGTTCTGAAGCAAGG	This study
rcsB RT RP	GACGTAATACTTCGCTCTCTTTAGG	This study
proC RT FP2	CTCGGTCACGCCCAATGC	This study
proC RT RP2	CATGGCTTCAATGAACATAAACACG	This study
ffh RT FP2	AACTGGTTGCGGCGATGG	This study
ffh RT RP2	CTTACCCACACTGGTGGTTTTAC	This study
Probe	Sequence	Source or Reference
rcsD	CCACGACATTGAGATAGCCGCAGCC	This study
rcsB	ACGCTTATCGCCATAACCGCCG	This study
proC	TGCCGAACCACTCACGCCTACCACG	This study
ffh	CCGCCATCAGCACGACAGCCG	This study

A

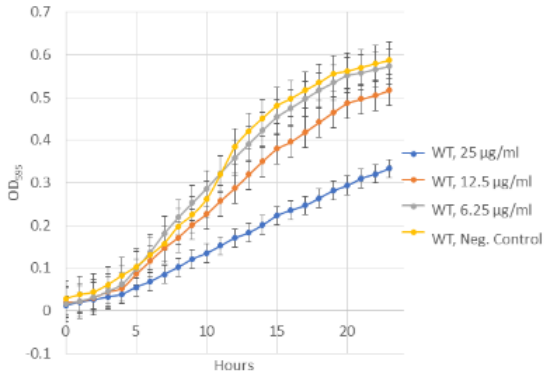

B

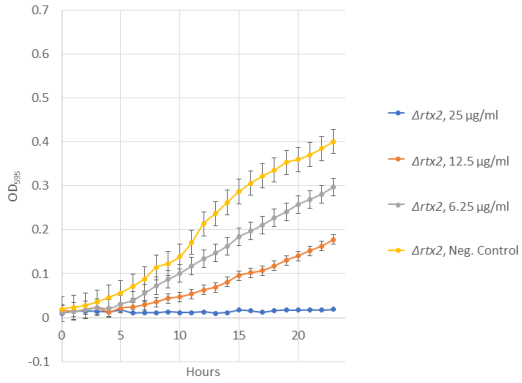

C

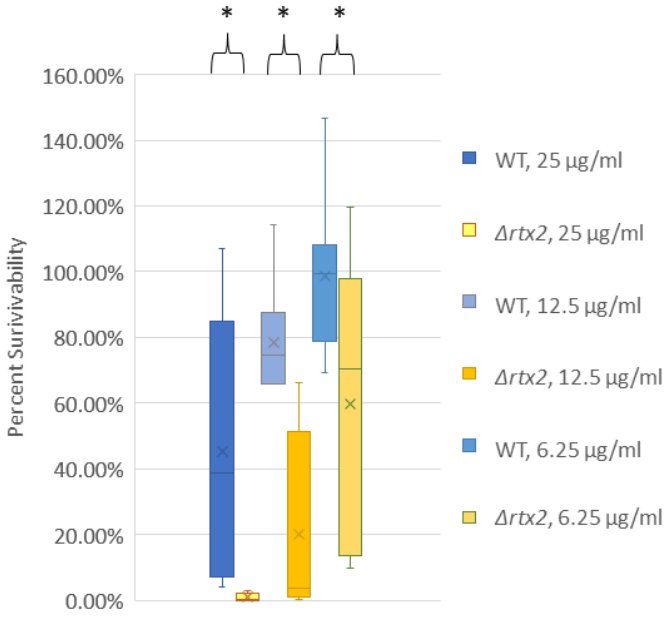

Figure A.1. Deletion of *rtx2* increases sensitivity to Polymyxin B. Both A) wild type and B) *Δrtx2* strains were incubated statically overnight against varying concentrations of the cell envelope targeting antibiotic Polymyxin B**.** Error Bars denote Standard Error C) Endpoint plate counts showed the Δ*rtx2* mutant had increased sensitivity to Polymyxin B versus the wild type. * indicates treatments that are statistically different at P≤0.05 by t-test. Results are based on 3 biological replicates, each with 3 technical replicates.

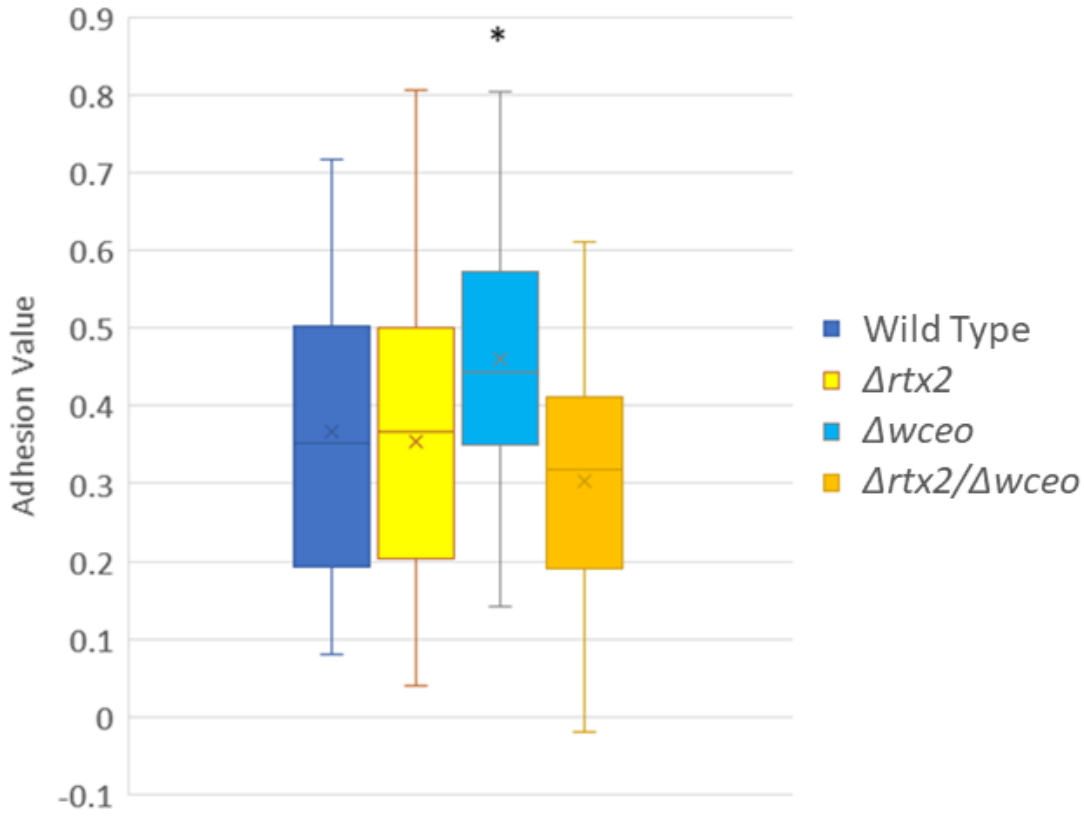

Figure A.2. Deletion of *rtx2* decreases surface adhesion *in vitro*. Surface Adhesion Crystal Violet Assays with poly-L-lysine coated microplates showed that the deletion of *rtx2* reduces surface adhesion in a non-EPS producing (Δ*wceo*) genetic background. Adhesion value or Specific Biofilm formation (SBF) is: growth normalized biofilm accumulation was calculated as follows: (OD595CV-media value)/(OD595Cell growth-media value)(Niu and Gilbert, 2004). * indicates statistically different results based on a Linear Regression Model ($p < 0.01$). Results are based on 5 biological replicates, each with no less than 5 technical replicates.

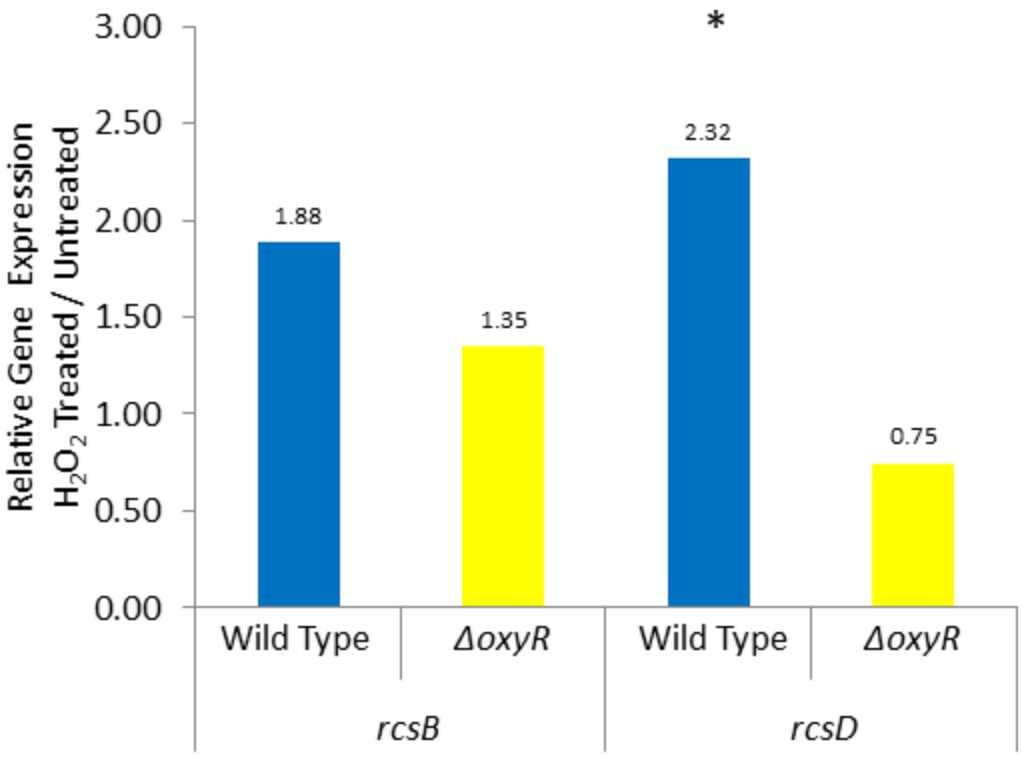

Figure A.3. **Expression of *rcsD* is induced by H_2O_2.**Exposure to 10 µM H_2O_2 for 5 minutes. Only wild type *P. stewartii* had increased *rcsD* expression after 5 minutes. *P. stewartii* was grown in Luria broth with 0.2% glucose. Asterisk symbolize treatments that are statistically different at P≤0.05 by t-test.

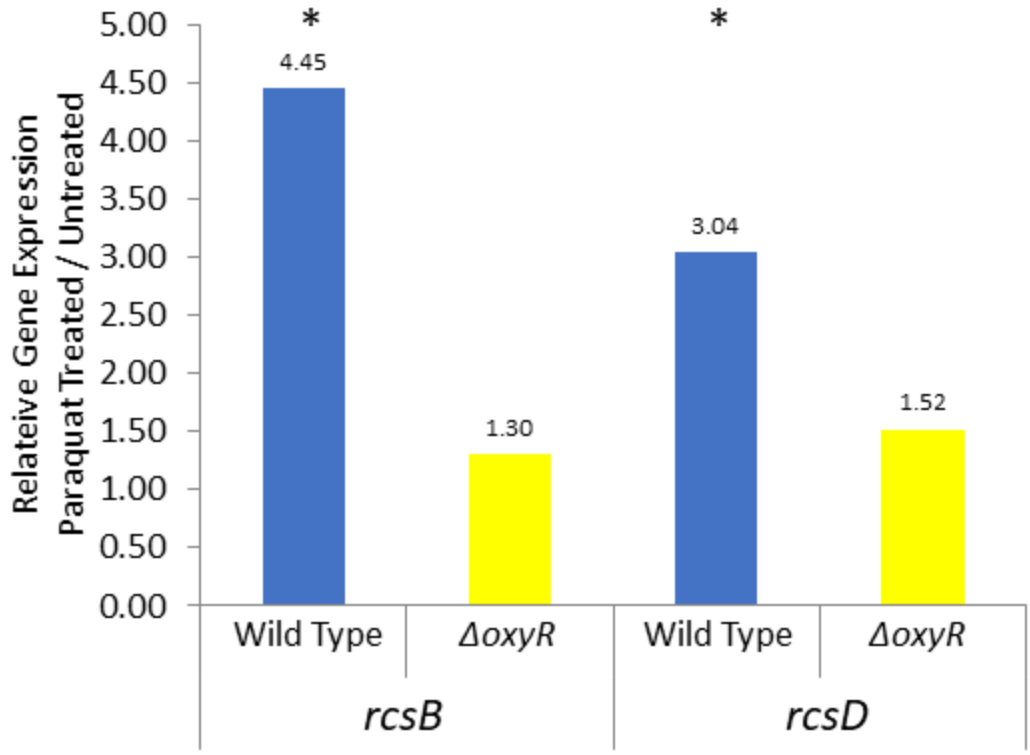

Figure A.4. ROS induces expression of components of the Rcs phosphorelay. Induction of expression of *rcsB* and *rcsD* when exposed to 0.2 µg/ml of paraquat for 15 minutes, wild type *P. stewartii* showed significant induction of gene expression of these two genes compared to Δ*oxyR* after exposure for 15 minutes. The gene *rcsD* encodes the phosphotransfer receptor RcsD, while *rcsB* encodes for the terminal response regulator RcsB. Asterisk symbolize treatments that are statistically different at P≤ 0.05 by t-test. *P. stewartii* was grown in Luria broth with 0.2% glucose.

Literature Cited

Burbank, L. and Roper, M.C. 2014. OxyR and SoxR Modulate the Inducible Oxidative Stress Response and Are Implicated During Different Stages of Infection for the Bacterial Phytopathogen *Pantoea stewartii* subsp. *stewartii*. *Molecular Plant-Microbe Interactions* 27(5): 479-490.

Clark, J. D., and Maaloe, O. 1967. DNA replication and the cell division cycle in *Escherichia coli*. *Journal of Molecular Biology* 23:99-112.

Koutsoudis, M.D., Tsaltas, D., Minogue, T.D., and Von Bodman, S.B. 2006. Quorum-sensing regulation governs bacterial adhesion, biofilm development, and host colonization in *Pantoea stewartii* subspecies *stewartii*. *Proceedings of the National Academy of Sciences* 103: 15 5983-5988

Niu, C., and Gilbert, E.S. 2004. Colorimetric Method for Identifying Plant Essential Oil Components That Affect Biofilm Formation and Structure. *Applied and Environmental Microbiology* 70(12): 6951-6956.

Roper, M.C., Burbank, L.P., Williams, K., Viravathana, P., Tien, H. and Von Bodman, S. 2015. A large repetitive RTX-like protein mediates water-soaked lesion development, leakage of plant cell content and host colonization in the *Pantoea stewartii* subsp. *stewartii* pathosystem. *Molecular Plant-Microbe Interactions* 12: 1374-1882.

Takle, G. W., Toth, I. K., and Brurberg, M. B. 2007. Evaluation of reference genes for real-time RT-PCR expression studies in the plant pathogen *Pectobacterium atrosepticum*. BMC Plant Biology. 7:50

Theunissen, S., De Smet, L., Dansercoer, A., Motte, B., Coenye, T., Van Beeumen, J.J., Devreese, B., Savvides, S.N., Vergauwen, B. 2010. The 285 kDa Bap/RTX hybrid cell surface protein (SO4317) of *Shewanella oneidensis* MR-1 is a key mediator of biofilm formation. *Research in Microbiology* 161: 144-152.